OPEN EUROPEAN JOURNAL ON VARIABLE STARS
March 2011 http://var.astro.cz/oejv ISSN 1801-5964

NEW VARIABLE STARS DISCOVERED FROM THE WESTERN ITALIAN ALPS. I.
OBSERVATIONS FROM FIELDS 12hr < RA < 24hr

Mario Damasso[1,2], Paolo Giacobbe[3], Giorgio Toso[1], Paolo Calcidese[1], Andrea Bernagozzi[1], Enzo Bertolini[1], Alessandro Sozzetti[4], Mario G. Lattanzi[4], Matteo Perdoncin[5], and R. Smart[4]

1) Osservatorio Astronomico della Regione Autonoma Valle d'Aosta, Fraz. Lignan 39, 11020, Nus (AO), Italy (www.oavda.it). E-mail of the corresponding author: m.damasso@gmail.com

2) Dipartimento di Astronomia, Università di Padova, Vicolo dell'Osservatorio 3, 35122, Padova, Italy

3) Dipartimento di Fisica, Università di Trieste, Via Tiepolo 11, 34131, Trieste, Italy

4) INAF – Osservatorio Astronomico di Torino, Via Osservatorio, 20, 10025 Pino Torinese (Torino), Italy

5) Dipartimento di Fisica - Università di Torino, via Pietro Giuria 1, I-10125, Torino, Italy

Abstract: We present 20 new variable stars discovered at the Astronomical Observatory of the Autonomous Region of the Aosta Valley in the course of observations carried out from April to October 2010. The list of the newly discovered stars comprises 19 pulsating variables (two of them should be classified as Delta Scuti and 16 as Mira Ceti-type/Semi-Regular pulsators), and one W UMa eclipsing binary system. Our proposed variability classification relies on the properties of the optical differential light curves that we obtained using less than 1-meter class telescopes.

---

1. INTRODUCTION

We announce the discovery of 20 new variable stars (19 pulsating stars and one eclipsing binary system). The data discussed here are based on observations carried out at the Astronomical Observatory of the Autonomous Region of the Aosta Valley (OAVdA), in the Western Italian Alps, from April to October 2010, using less than 1-meter class optical telescopes. These data are only a part of our conspicuous database of photometric measurements collected since December 2009, and other new variable stars that we found will be published in a second paper (Giacobbe et al., in preparation). On December 2009 we started a one-year-long photometric survey of a small sample of nearby M dwarfs with the main goal of monitoring their optical microvariability over a period of several weeks, to assess in particular the implications for the detection of small-size transiting planets. This observing campaign, which we defined as a 'pilot study', represents a preparatory step toward the beginning of the project APACHE (A PAthway towards the Characterization of Habitable Earths), a new long-term survey of thousands of red dwarfs in the northern-emisphere aimed at the detection of rocky planets using the photometric transit method (Damasso et al., 2011). The variables discussed here are stars which were present in the target fields observed during the pilot study.

2. INSTRUMENTATION AND METHODOLOGY

The observations for the pilot study were carried out using three small-class optical telescopes equipped with CCD cameras. Their main characteristics are summarized in Table 1. Every instrument was equipped with a set of BVRI standard filters. The data coming from the 250mm telescope were collected using an I filter, while the 400 and 810mm telescopes made use of R filters. This choice of the filters is a consequence of the primary aim of our survey, i.e. the photometric monitoring of red dwarfs. In this paper we discuss data collected with the 250 and 810mm telescopes, while in Giacobbe et al. (in preparation), where results from fields 00hr < AR < 12hr are presented, also data from the 400mm are shown.

The reduction and analysis of the CCD images were performed by the software package TEEPEE (Transiting ExoplanEts PipElinE) developed by the authors. A detailed description of the first version of

the TEEPEE pipeline, containing the basic functions preserved in the updated versions, is given in Damasso et al. (2010). The final result of the data processing is the generation of the differential light curves, obtained making use of aperture photometry, of all the stars in the CCD field which were automatically recognized in every frame of the series. In this way we were able to identify the variable stars present in each field after a visual inspection of the light curves. On the Y-axis of each light curve is indicated the differential magnitude obtained as the difference between the average instrumental magnitude of the selected comparison stars and the instrumental magnitude of the target. Using this convention, epochs of minimal differential magnitudes correspond to epochs of minimal brightness of the target.
The variables presented here showed a clear (or at least unambiguous) photometric behavior easily ascribable to one of the GCVS variability types. We discarded the objects with a low S/N ratio, the ones showing a type of variability not easy to classify or transit-like signals recorded at only one epoch, which are unuseful to determine the orbital period of the eclipsing system.
The updated version of TEEPEE package used to process the data is improved concerning the methods for the selection of the optimal aperture radius and set of reference stars for each observing session. Up to 12 different apertures are tested and the best set of comparison stars is automatically determined from a list of the 100 brightest objects in the field, excluding the ones too close to the CCD borders. The method we used to determine the best set of comparisons consists primarily in sorting the list of the possible 100 reference stars on the base of the RMS of their light curves, obtained from differential photometry with the other 99 candidate references. The aperture and set of reference stars selected at the end of the data processing are the ones which give the smallest RMS for the entire light curve of the object of interest. This means that the set of the best comparison stars found automatically changes on nightly basis for a particular object, and we did not use the same ensemble of comparisons for each observing session. That is the reason why we do not provide here the reference stars for each target.

In § 3.2 we discuss variables which show periods longer than 30 days. For these stars we produced light curves relative to the whole period of observation (66 days), obtained running TEEPEE over all the nights at once, i.e. treated as they were a single (long) observing session. The differential photometry was automatically performed on both newly discovered and already known variables using the best set composed of 39 comparison stars, which are detailed in Table 3.

The time series analysis of the light curves has been performed using two computer programs. One is PERIOD04 (http://www.univie.ac.at/tops/Period04/), which is a software to perform discrete Fourier transformation. Denoting with ω_i a significant frequency calculated with the Fourier decomposition, with A_i the corresponding amplitude of the frequency peak in the periodogram, and with φ_i the phase constant, the light curve of a target can be approximated, for each value of time t, with the analytical function $F(t) = C + \Sigma A_i [\sin(2\pi(\omega_i t + \varphi_i)]$, where C is a zero-point constant and the sum is over all the significant frequencies calculated.
The second software is the PERIOD Time-Series Analysis Package (version 5.0; http://www.starlink.rl.ac.uk/star/docs/sun167.htx/sun167.html), which is a part of the STARLINK project, for analysis with the Lomb-Scargle algorithm implemented in for astronomical data processing (http://starlink.jach.hawaii.edu/starlink). The uncertainties in the variability periods which we report are internal minimum errors as evaluated by the software.

For some variables we performed a sinusoidal fit to their light curves, which we show in the plots. The fit algorithm used is implemented in the PERIOD package, fixing the period of the sine function to the one evaluated with the Lomb-Scargle procedure.

3. RESULTS AND DISCUSSION ON THE NEW VARIABLE STARS

The type of variability that we suggest for each object is necessarily based only on the characteristics showed by its differential light curve, because the discovery of such variables emerged from data collected for a different purpose and could not be improved with follow-up observations.
To confirm that our findings are really new variable stars, we checked the following Web-based catalogues: VizieR (http://vizier.u-strasbg.fr/), the International Variable Star Index

(http://www.aavso.org/vsx/index.php), the General Catalogue of Variable Stars (http://www.sai.msu.su/groups/cluster/gcvs/gcvs/), and the ASAS catalogue of variable stars (http://www.astrouw.edu.pl/asas/?page=acvs).

We adopted the books of Sterken and Jaschek (1996), Percy (2007) and Aerts et al. (2010) as the main resources to propose a classification for the new variable stars we observed.
The types of variability are coded according the GCVS classification. For each object we adopted the standard magnitudes reported by the NOMAD-1 catalogue, without correcting for absorption.

Table 2 summarizes the main information about the new variables found, including the suggested types of variability and the periods we were able to evaluate for the stars which clearly show periodical changes in their light curves.
In the following sections we discuss each variable star separately, according the order in Table 2. We divide the discussion in four paragraphs, each devoted to a particular field.

3.1 NOMAD-1 1367-0306809

This object was monitored for 13 nights starting from May 24th until July 18th, 2010, using the 250mm telescope. Due to its V~14 magnitude and the small aperture of the telescope, the quality of the data for this star is not so good as for other targets in the field. We performed Fourier decomposition of the photometric time series, which then appears to be consistent with that of a pulsating star. We found 2 significant frequencies: F1=5.78616777 cycle/day (corresponding to a period P=0.172826 days), and F2=3.42487131 cycle/day (corresponding to a period P=0.291982 days). The frequency F2 represents the peak value in the periodogram calculated over the residuals O-C, obtained from the difference between the observed data points and the corresponding ones calculated with a sinusoidal fit using F1. The corresponding amplitudes and phase factors for F1 and F2 are: A1=0.0162772765, Φ1=0.19464, A2=0.0170448468, Φ2=0.386117. The zero-point factor is C=0.994236538. In Fig. 1 we show the original light curve folded according the frequency F1 (plot a), the corresponding periodogram (plot b), the residuals O-C, folded according to the frequency F2 (plot c), and the frequency content of the residuals (plot d).
On the base of our data and the color information available from catalogues, we can not suggest a specific classification for this variable, only considering it a stellar pulsator with a good confidence.

3.2 A FIELD RICH OF MIRA AND SEMI-REGULAR VARIABLES

The new variable stars grouped in this paragraph were discovered in a field rich of red variables already reported in literature. In Fig. 2 we show the light curves that we obtained from our data for the known Mira-type variables KR Sge, LL Sge, LM Sge, LV Sge, LX Sge (Rosino and Guzzi, 1978), NSVS J1914429+190818 (Woźniak et al., 2004), and for the slow irregular L variable NSVS J1913242+192533 (Woźniak et al., 2004). On the AAVSO site, the latter object is suggested to have a period of 68 days which our data do not show, strengthening the hypothesis that this target is an irregular L variable.
In order to support our hypothesis concerning the classification of the new stars discussed in this section, for comparison we report the color indexes of some of the Mira-type variables already known in the field (from NOMAD-1 photometry): V-J=10.953, V-H=12.227, V-K=12.966 (LL Sge); V-J=7.289, V-H=8.487, V-K=8.927 (LM Sge); V-J=10.469, V-H=11.727, V-K=12.464 (LV Sge); V-J=8.551, V-H=9.663, V-K=10.269 (LX Sge).
All the data from this field were collected using the 250mm telescope during observations spanning 66 days. The periods that we suggest for the new long-period variables should all be considered as tentative. The periodograms have been calculated assuming as the maximum frequency the Nyquist frequency (F_N=724 cycle/day), and no significant peaks are present out of the frequency range selected for the plots (from 0 to 10 cycle/day).

3.2.1 NOMAD-1 1095-0380434

This is probably a red giant star with color indexes V-J=6.008, V-H=7.118 and V-K=7.53. Fig. 3 shows the data for this object, which appears to be a SR (Semi-Regular) pulsating star with an estimated period P~39 days and a peak-to-peak amplitude of ~0.056 mag (as estimated from a sinusoidal fit). The data are folded according the ephemeris HJD (phase=0) = 2,455,371.51438 + P*N.

3.2.2 NOMAD-1 1093-0380200
This is a highly red star with color indexes V-J=9.047, V-H=10.352 and V-K=11.134. Fig. 4 shows the light curve for this star, which is very similar to the one observed for the Mira-type star LV Sge (Fig. 2) and is characterized by a steady dimming of nearly 1 mag over two months. We suggest for this star a classification as a Mira or SR variable.

3.2.3 NOMAD-1 1095-0380572
This is probably a red giant star with color indexes V-J=7.698, V-H=8.874 and V-K=9.378. Fig. 5 shows the data for this object, for which we may suggest a classification as SR pulsating star. The peak-to-peak amplitude is ~0.33 mag, as estimated from a sinusoidal fit.

3.2.4 NOMAD-1 1095-0381014
This is probably a red giant star with color indexes V-J=7.548, V-H=8.672 and V-K=9.148. Fig. 6 shows the data for this object, which appears to be a SR pulsating star with a tentative period P~54 days and a peak-to-peak amplitude of ~0.2 mag (as estimated from a sinusoidal fit). The data are folded according the ephemeris HJD (phase=0) = 2,455,371.51438 + P*N.

3.2.5 NOMAD-1 1095-0381250
This is probably a red giant star with color indexes V-J=7.559, V-H=8.701 and V-K=9.156. Fig. 7 shows the data for this object, which does not show a periodicity less than 66 days. This star may be classified as a Mira or SR variable.

3.2.6 NOMAD-1 1090-0387525
This is probably a red giant star with color indexes V-J=7.461, V-H=8.628 and V-K=9.124. Fig. 8 shows the data for this object, which appears to be a SR pulsating star with an estimated period P~42 days and a peak-to-peak amplitude of ~0.24 mag (as estimated from a sinusoidal fit). The data are folded according the ephemeris HJD (phase=0) = 2,455,371.51438 + P*N.

3.2.7 NOMAD-1 1093-0381534
This is probably a red giant star with color indexes V-J=8.404, V-H=9.589 and V-K=10.108. In Fig. 9 the light curve is showed, which does not show a periodicity less than 66 days. This star may be classified as a Mira or SR variable.

3.2.8 NOMAD-1 1095-0382124
This is probably a red giant star with color indexes V-J=7.182, V-H=8.367 and V-K=8.842. Fig. 10 shows the data for this object, which appears to be a SR pulsating star with a tentative period P~54 days and a peak-to-peak amplitude of ~0.16 mag (as estimated from a sinusoidal fit). The data are folded according the ephemeris HJD (phase=0) = 2,455,371.51438 + P*N.

3.2.9 NOMAD-1 1090-0388621
This is a highly red star with color indexes V-J=10.823, V-H=12.102 and V-K=12.706. In Fig. 11 the light curve is showed, which does not show a clear periodicity less than 66 days. This star could be classified as a Mira or SR variable.

3.2.10 NOMAD-1 1091-0387997
This is probably a red giant star with color indexes V-J=8.163, V-H=9.39 and V-K=9.893. Fig. 12 shows the data for this object, which may be a M/SR pulsating star.

3.2.11 NOMAD-1 1093-0382699
This is probably a red giant star with color indexes V-J=7.318, V-H=8.469 and V-K=9.0. Fig. 13 shows the data for this object, which may be a M/SR pulsating star with a tentative period P~63 days and a peak-to-peak amplitude of ~0.36 mag (as estimated from a sinusoidal fit). Data are folded according the ephemeris HJD (phase=0) = 2,455,371.51438 + P*N.

3.2.12 NOMAD-1 1090-0389865
This is probably a red star with color indexes V-J=8.021, V-H=9.27 and V-K=9.81. In Fig. 14 the light curve is showed, which does not show a clear periodicity less than 66 days. This star may be classified as a Mira or SR variable.

3.2.13 NOMAD-1 1094-0383234
This is probably a red giant star with color indexes V-J=6.008, V-H=7.118 and V-K=7.53. Fig. 15 shows the data for this object, which appears to be a SR pulsating star with a period P~45 days and a peak-to-peak amplitude of ~0.18 mag (as estimated from a sinusoidal fit). Data are folded according the ephemeris HJD (phase=0) = 2,455,371.51438 + P*N.

3.2.14 NOMAD-1 1092-0387428
This is a highly red star with color indexes V-J=8.542, V-H=9.682 and V-K=10.289. Fig. 16 shows the original light curve, which is very similar to the one of the star in Fig. 4 and is characterized by a monotonic dimming of nearly 1.2 mag over two months. We suggest for this star a classification as a Mira or SR variable.

3.2.15 NOMAD-1 1091-0389915
This is probably a red giant star with color indexes V-J=7.167, V-H=8.32 and V-K=8.781. Fig. 17 shows the data for this object, which appears to be a SR pulsating star with a tentative period P~62 days and a peak-to-peak amplitude of ~0.24mag (as estimated from a sinusoidal fit). The sinusoidal fit to this light curve reveals that its profile is asymmetric. Data are folded according the ephemeris
HJD (phase=0) = 2,455,371.51438 + P*N.

3.2.16 NOMAD-1 1092-0388944
This is probably a red giant star with color indexes V-J=6.504, V-H=7.713 and V-K=8.168. Fig. 18 shows the data for this object, which appears to be a SR pulsating star with some changes in the amplitude of the light curve. From our data we can only guess a possible periodicity of ~30 days. It is probably a SRb variable, but it would be necessary to observe more cycles in order to properly define its variability type.

3.3 NOMAD-1 1077-0767537
This star was observed with the 250mm telescope. We performed Fourier decomposition of the light curve, finding 2 significant frequencies: F1=7.45248337 cycle/day (corresponding to a period P=0.134183 days), and F2=4.52912947 cycle/day (corresponding to a period P=0.220793 days). The frequency F2 corresponds to the peak value in the periodogram calculated over the residuals O-C, obtained from the difference between the observed data points and the corresponding ones calculated with a sinusoidal fit using F1. The corresponding amplitudes and phase constants are: A1=0.072678217, Φ1=0.492082, A2=0.0247829231, Φ2=0.99022. The zero-point factor is C=1.00239438. In Fig. 19 we show the light curve folded according the frequency F1 (plot a), the corresponding periodogram (plot b), the residuals O-C, folded according the frequency F2 (plot c), and the periodogram with the frequency content of the residuals (plot d). Considering that the peak-to-peak amplitude is ~0.15 mag and that this star is characterized by color indexes B-V=0.55, V-R=0.29, V-J=0.832 and V-K=1.18, which are compatible with a main sequence late-F star, we suggest for this pulsator a classification as a DSCT.

3.4 NOMAD-1 1617-0165649
This object was observed for 37 nights by the 810mm telescope and clearly shows the properties of an eclipsing binary of W UMa type. The estimated rotation period of the components is P=0.35517±0.00001 days. Fig. 20 shows the folded data (averaged in 200 bins), with ephemeris HJD = 2,455,440.54030+P*N. It is evident from the plot the presence of asymmetries close to the minima and maxima of the light curve. Fig. 21 shows four different epochs of observations which demonstrate that the shape of the light curve changed from epoch to epoch. This variability should be attributed to the presence of spotted regions on the surfaces of both stars. Our hypothesis is based on the fact that W Uma-type objects are usually heavily spotted systems, as theoretically predicted by Binnendijk (1970), who was the first to propose that dark spots exist on the surfaces of W UMa eclipsing binary systems to explain the asymmetry and variability of

the light curves at different epochs, and later demonstrated by doppler imaging (see for instance Hendry & Mochnacki, 2000).

3.5 NOMAD-1 1616-0162705

This object was observed for 37 nights by the 810mm telescope and it appears to be a purely radial pulsator with a period P=0.10073±0.00001 days. In Fig. 22 we show the folded light curve (80 bins), according the ephemeris HJD (min)=2,455,482.39845+P*N, and the periodogram. The shape of the curve appears highly symmetric and the peak-to-peak amplitude is ~0.033 mag (evaluated with a sinusoidal fit, which is superposed to the data in the first panel of Fig. 22). The color indexes are B-V=0.68, V-J=1.058 and V-K=1.361 which, taking into account the reddening, are compatible with a very-late F main sequence star. We suggest that this star may be classified as a DSCT variable.

4. ACKNOWLEDGMENTS

MD, GT, PC, and AB are supported by grants provided by the European Union, the Autonomous Region of the Aosta Valley and the Italian Department for Work, Health and Pensions. The OAVdA is supported by the Regional Government of the Aosta Valley, the Town Municipality of Nus and the Mont Emilius Community. This research has made use of the SIMBAD database, operated at CDS, Strasbourg, France, and of the NASA Astrophysics Data System Bibliographic Services.
We thank the anonymous referee and Albino Carbognani (OAVdA and Observatoire de la Côte d'Azur) for useful comments to the manuscript.

5. BIBLIOGRAPHY

- Aerts, C., Christensen-Dalsgaard, J., and Kurtz, D. W., 2010, Asteroseismology, Springer
- Binnendijk, L., 1970, The orbital elements of W Ursae Majoris systems (1970VA.....12..217B)
- Damasso, M., et al., 2010, Photometric transit search for planets around cool stars from the Western Italian Alps: a site characterization study (2010PASP..122.1077D)
- Damasso, M., et al., 2011, A microvariability study of nearby M dwarfs from the Western Italian Alps: status update, to appear in the Proceedings of the IAU Symposium 276 'The Astrophysics of Planetary Systems: Formation, Structure, and Dynamical Evolution'
- Giacobbe, P., et al., 2011, New variable stars discovered from the Western Italian Alps. II. Observations from fields 00hr < RA < 12hr, in preparation
- Hendry, P. D., and Mochnacki, S., 2000, Doppler Imaging of VW Cephei: Distribution and Evolution of Starspots on a Contact Binary (2000ApJ...531..467H)
- Percy, J.R., 2007, Understanding Variable Stars, Cambridge University Press
- Rosino, L., Guzzi, L., 1978, Infrared variable stars in the Milky Way field at R.A. 19h16m - Dec. +18° 28' (1950) (1978A&AS...31..313R)
- Sterken, C., Jaschek, C. (Eds.), 1996, Light Curves of Variable Stars. A Pictorial Atlas, Cambridge University Press
- Woźniak, P. R., et al., 2004, Identifying Red Variables in the Northern Sky Variability Survey (2004AJ....128.2965W)

Table 1 – Summary of the main characteristics of the telescope systems used in OAVdA for the pilot study, a preparatory campaign for the upcoming APACHE survey.

	Telescope		CCD camera		Resulting configuration	
Optical scheme	Aperture (mm)	Focal ratio	Sensor area (pixel)	Pixel area (μm)	FoV (arcmin)	Plate scale ($''$/pixel)
Reflector Maksutov	250	f/3.80	2184×1472	6.8×6.8	52.10×35.11	1.43 (binning 1×1)
Reflector Ritchey-Chrétien	400	f/7.64	1024×1024	24×24	26.4×26.4	1.55 (binning 1×1)
Reflector Ritchey-Chrétien	810	f/7.90	2048×2048	15×15	16.3×16.3	0.48 (binning 1×1)

Table 2 – Summary of the new variable stars discussed in this paper.

Star ID NOMAD-1	**Star ID GSC2.3**	**RA (J2000)**	**DEC (J2000)**	**Vmag (NOMAD-1)**	**Types of suggested variability (GCVS codes)**	**Delta mag R (mag)***	**Estimated period (days)****
1367-0306809	N4CJ000080	17:54:04	46:42:04	13.84	pulsator	~0.05	0.172826 (frequency F1) 0.2919818 (frequency F2)
1095-0380434	N26S095788	19:12:46	19:31:42	14.66	SR	0.056	~39
1093-0380200	N26S074080	19:12:49	19:20:49	16.88 (GSC2.3)	M/SR	~0.8	-
1095-0380572	N26S094790	19:12:51	19:31:11	17.97	SR	0.33	-
1095-0381014	N26S096123	19:13:08	19:31:58	15.99	SR	0.2	~53
1095-0381250	N26S094065	19:13:17	19:30:38	16.01	M/SR	0.31	-
1090-0387525	N26S044948	19:13:24	19:04:44	17.97	SR	0.24	~42
1093-0381534	N26S071251	19:13:42	19:19:10	16.9	M/SR	~0.29	-
1095-0382124	N26V001429	19:13:52	19:32:36	16.54	SR	0.16	~55
1090-0388621	N26S041190	19:14:01	19:02:13	17.59	M/SR	0.31	-
1091-0387997	N26S055576	19:14:22	19:10:56	17.05	M/SR	0.38	-
1093-0382699	N26S070220	19:14:29	19:18:49	16.5	SR	0.36	~63
1090-0389865	N26S045637	19:14:42	19:05:09	16.21	M/SR	~0.27	-
1094-0383234	N26S090324	19:14:49	19:29:04	16.86	SR	0.18	~45
1092-0387428	N26S068589	19:15:13	19:17:57	17.97	M/SR	~1.3	-
1091-0389915	N26S047973	19:15:31	19:06:31	15.05	SR	0.24	~62
1092-0388944	N26S060821	19:16:06	19:13:41	15.93	SR(b)	~0.11	close to 30 days?
1077-0767537	N0LW000410	22:40:30	17:43:59	14.3	DSCT	0.15	0.134183 (frequency F1) 0.220793 (frequency F2)
1617-0165649	N0WB000244	23:05:55	71:44:20	13.58	EW	0.42	0.35517±0.00001
1616-0162705	N0WB000269	23:07:12	71:40:27	13.1	DSCT	0.033	0.10073±0.00001

*For the long-period variables, this represents the magnitude range for the epochs spanning 66 days. For the variables for which we performed a sine fit we provide the estimated peak-to-peak amplitude.
**For the long-period variables, these represent tentative estimations assuming constant periods.

Table 3 – Summary of the comparison stars used to produce the aperture differential light curves in § 3.2.

Star ID	RA (J2000)	DEC (J2000)
HD 179585	19:12:26	19:12:30
NOMAD-1 1094-0380020	19:12:48	19:27:50
HD 349865	19:12:49	19:14:09
NOMAD-1 1093-0380254	19:12:51	19:23:30
NOMAD-1 1093-0380321	19:12:54	19:23:43
NOMAD-1 1095-0380824	19:13:01	19:32:08
HD 230897	19:13:03	19:27:54
NOMAD-1 1092-0383952	19:13:06	19:17:10
HD 349866	19:13:10	19:06:17
NOMAD-1 1091-0386017	19:13:12	19:08:52
NOMAD-1 1094-0380742	19:13:17	19:27:03
NOMAD-1 1092-0384276	19:13:18	19:14:33
NOMAD-1 1095-0381269	19:13:18	19:34:24
NOMAD-1 1094-0380805	19:13:19	19:24:19
NOMAD-1 1092-0384504	19:13:27	19:13:28
HD 230917	19:13:27	19:16:44
NOMAD-1 1090-0388005	19:13:40	19:04:51
NOMAD-1 1091-0386917	19:13:44	19:11:32
NOMAD-1 1094-0382002	19:14:02	19:27:02
HD 349904	19:14:05	19:25:51
HD 230964	19:14:19	19:23:15
NOMAD-1 1092-0385942	19:14:20	19:12:44
NOMAD-1 1092-0385932	19:14:20	19:13:35
NOMAD-1 1095-0382811	19:14:21	19:31:03
NOMAD-1 1093-0382587	19:14:24	19:20:57
NOMAD-1 1090-0389434	19:14:28	19:05:43
NOMAD-1 1094-0382867	19:14:35	19:28:42
NOMAD-1 1094-0382904	19:14:36	19:27:10
LHS 3446	19:14:39	19:18:21
NOMAD-1 1093-0382957	19:14:39	19:19:53
NOMAD-1 1093-0383117	19:14:45	19:18:48
NOMAD-1 1092-0386657	19:14:46	19:13:25
NOMAD-1 1090-0390061	19:14:48	19:03:42
NOMAD-1 1092-0387379	19:15:11	19:15:05
NOMAD-1 1091-0389571	19:15:18	19:11:16
HD 231005	19:15:22	19:02:06
NOMAD-1 1090-0391122	19:15:22	19:04:01
TYC 1607-1253-1	19:15:25	19:13:16

Figure 1 – (a) Light curve of the pulsating star NOMAD-1 1367-0306809 phased according the peak frequency F1=5.78616777 cycle/day. (b) Periodogram showing the frequency content of the original data. (c) Residuals O-C phased according the frequency F2=3.42487131 cycle/day, showing that they contain a significant periodicity. (d) Periodogram showing the frequency content of the residuals. (e) Finding chart for the target.

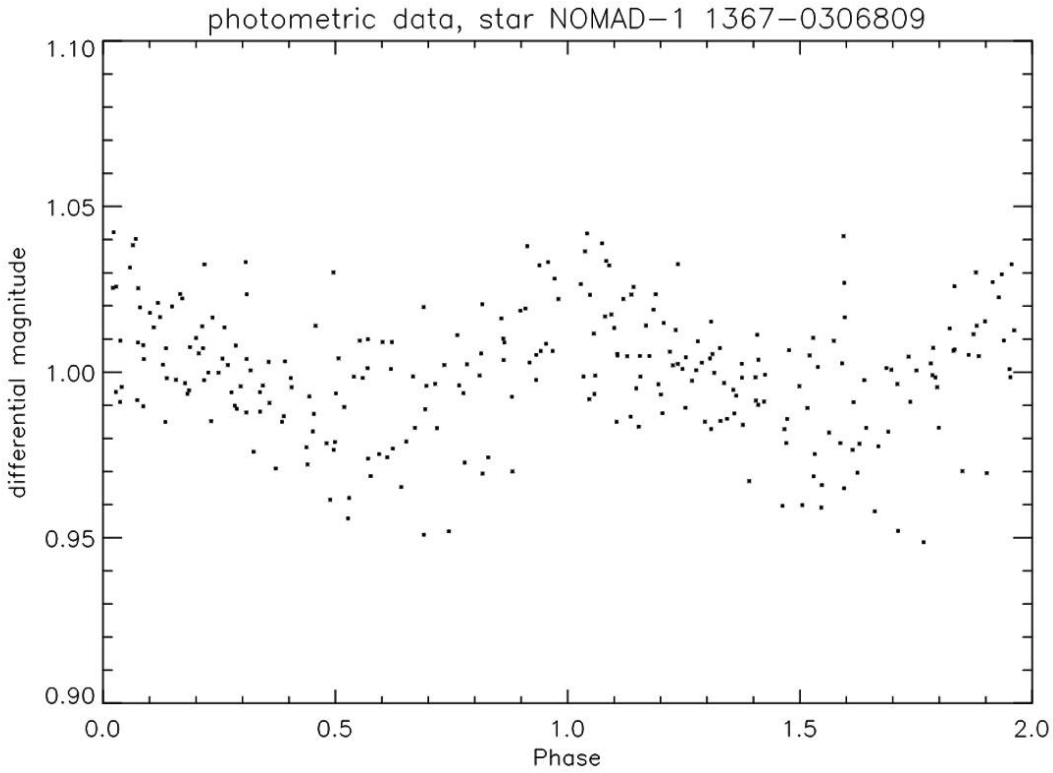

(a)

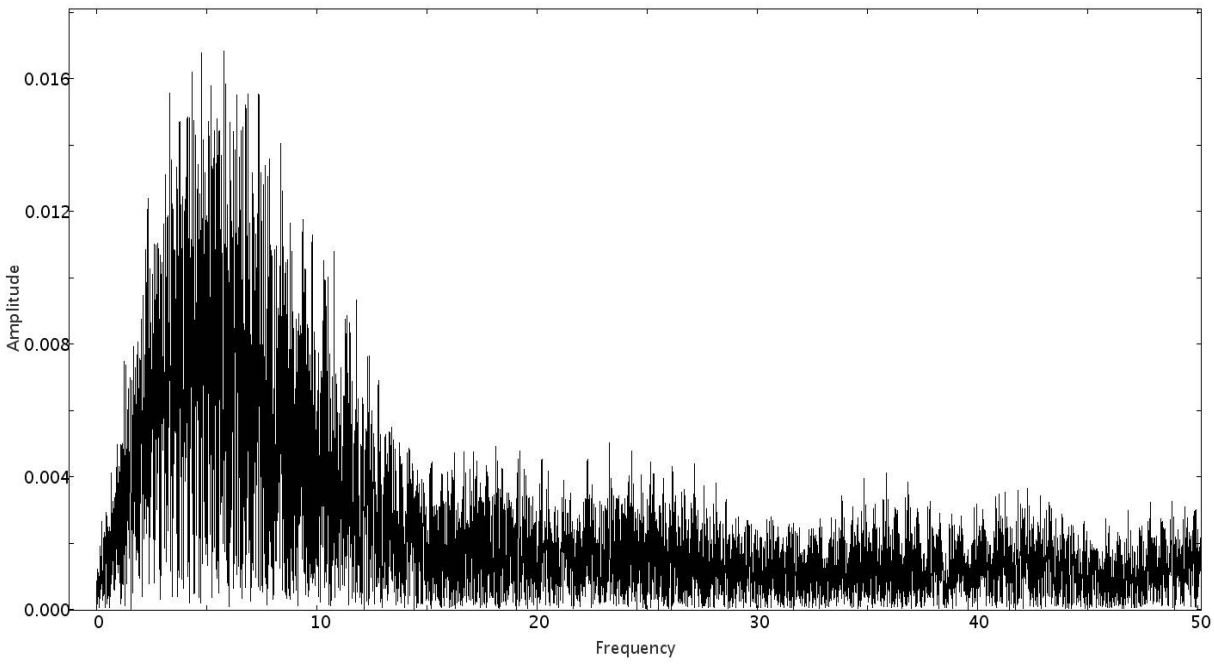

(b)

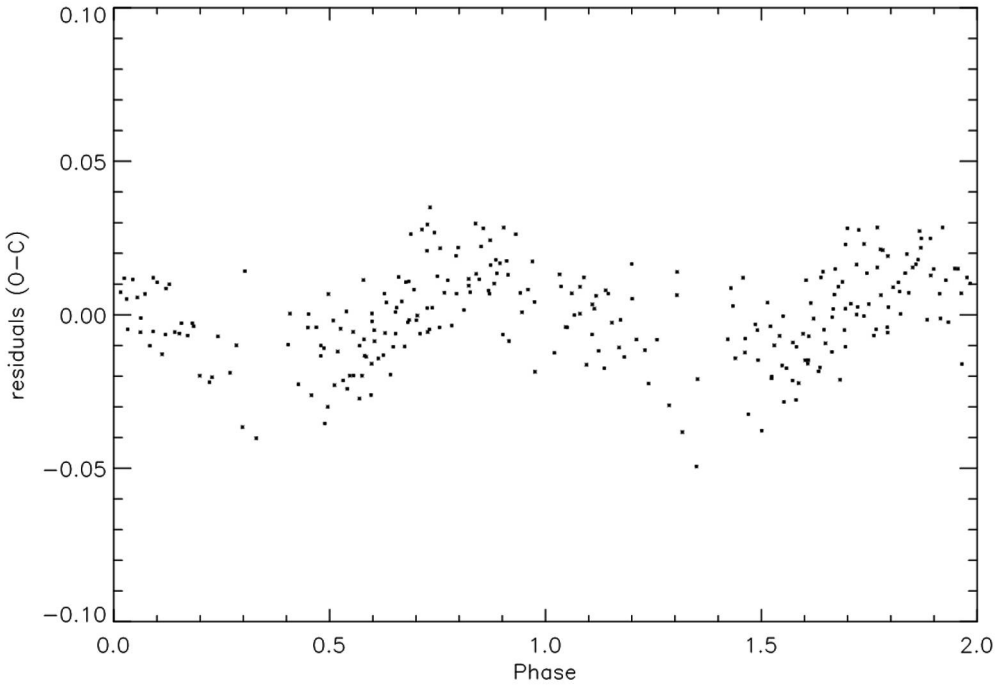
0.10
0.05
0.00
−0.05
−0.10
residuals (O−C)
0.0
0.5
1.0
1.5
2.0
Phase

(c)

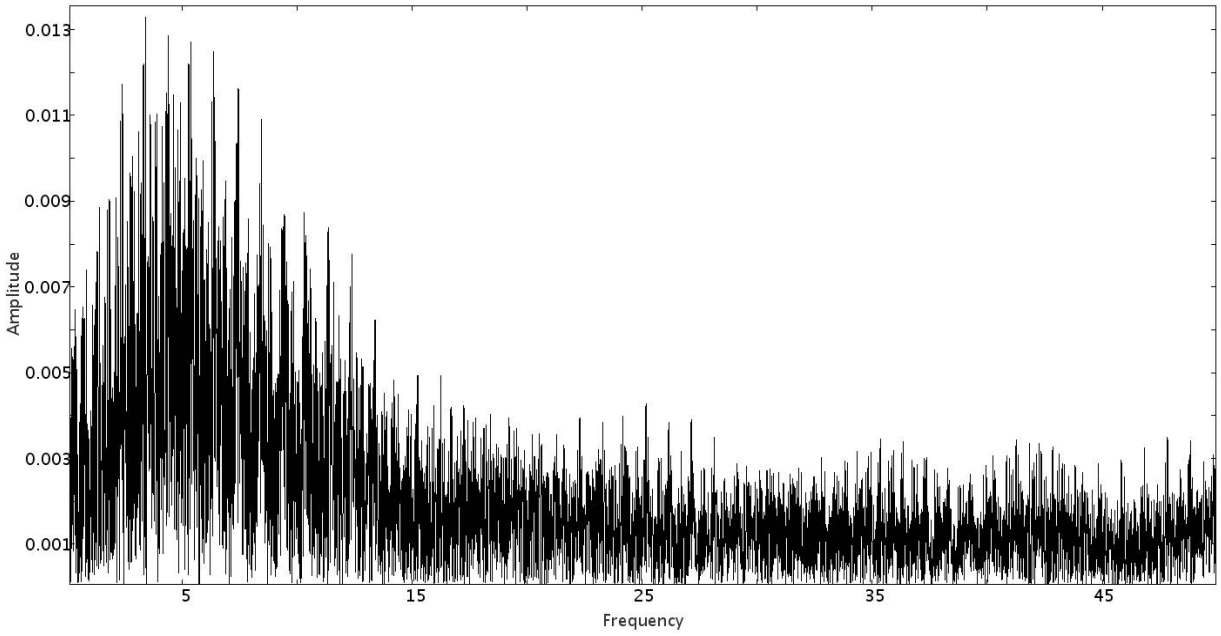
0.013
0.011
0.009
0.007
0.005
0.003
0.001
Amplitude
5
15
25
35
45
Frequency

(d)

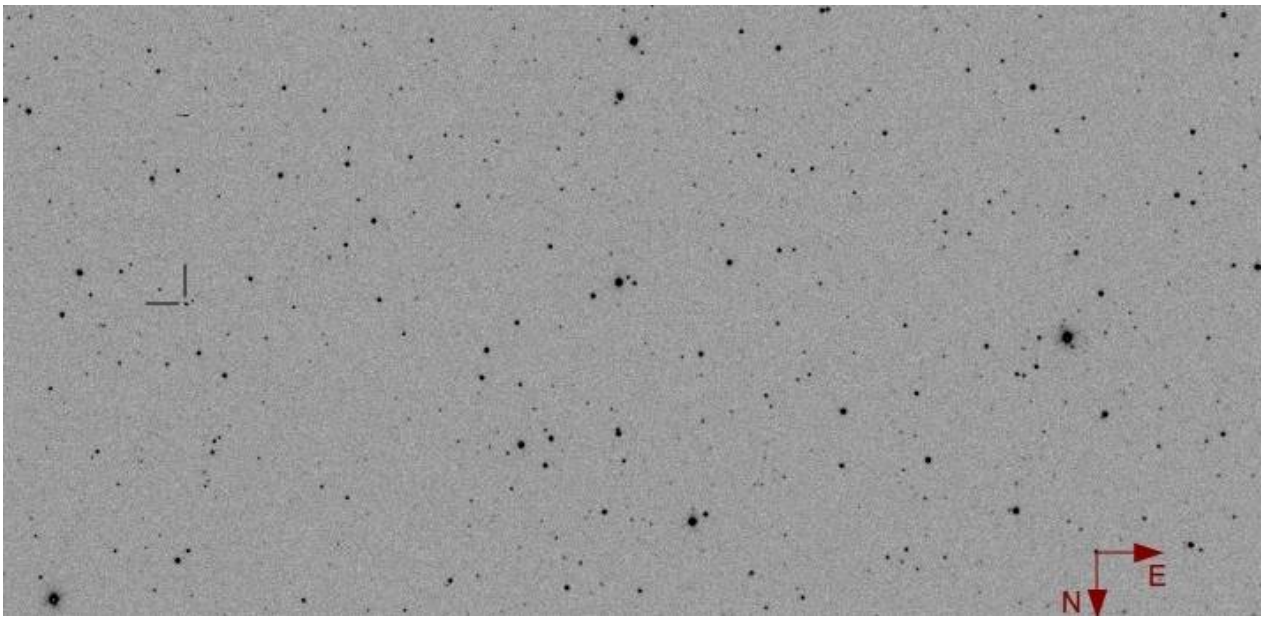

(e)

Figure 2 – Light curves of the known red variables KR Sge, LL Sge, LM Sge, LV Sge, LX Sge, NSVS J1913242+192533 and NSVS J1914429+190818. The quality of our data proves the reliability of the results provided by our pipeline TEEPEE.

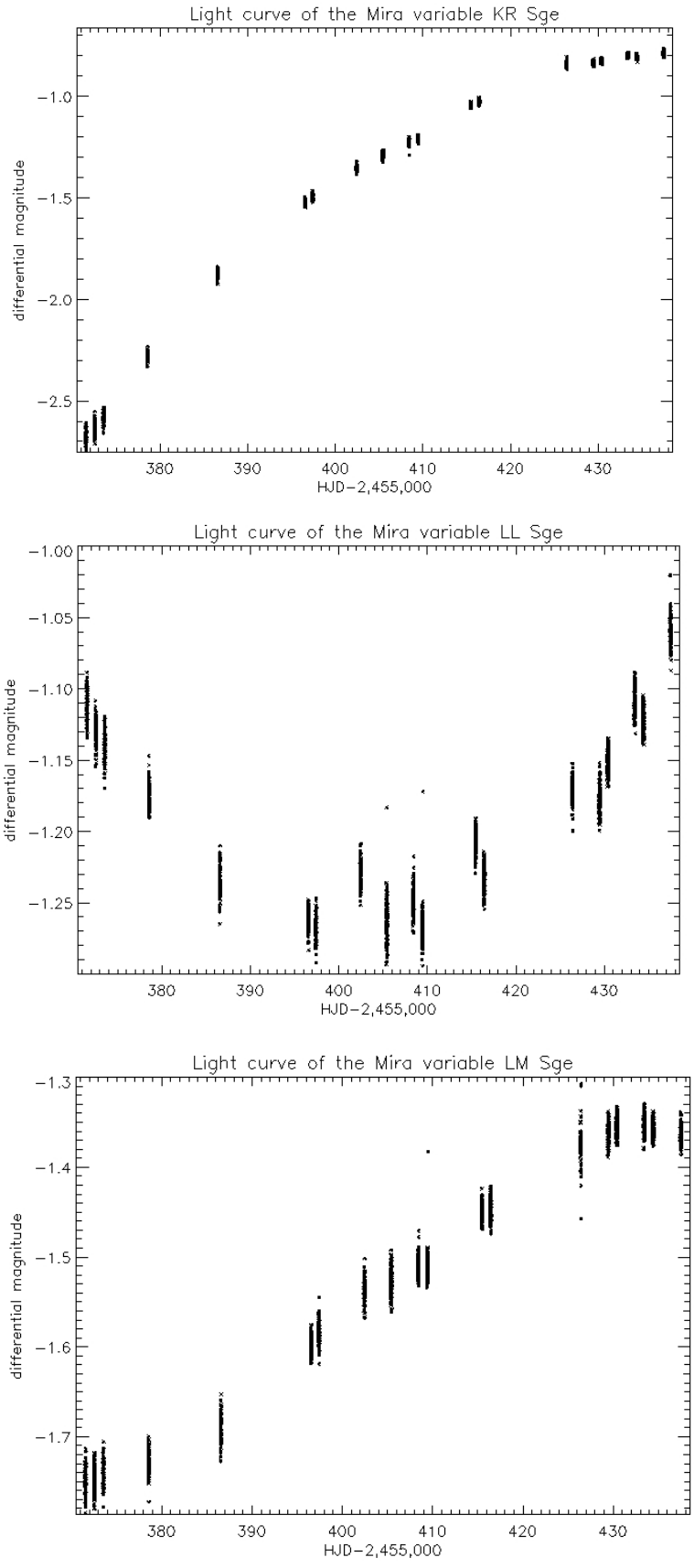

(Fig. 2 continued)

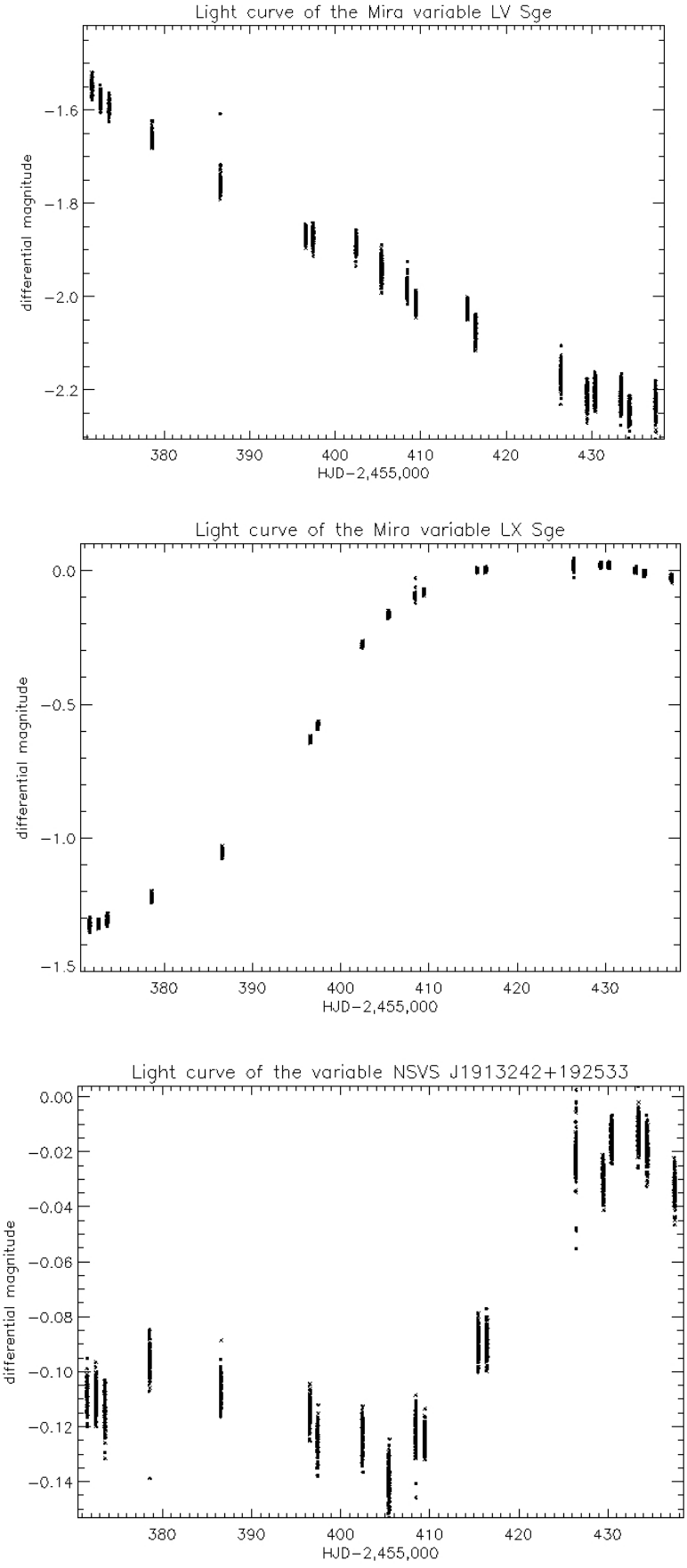

(Fig. 2 continued)

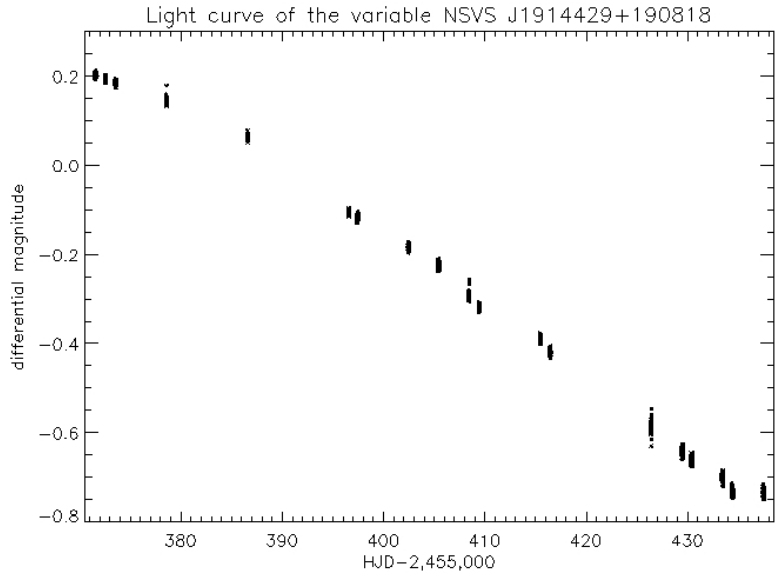

Figure 3 – (a) Original light curve of the star NOMAD-1 1095-0380434. (b) The phased light curve. Overplotted is the best fit sine curve. (c) The Lomb-Scargle periodogram. The peak frequency corresponds to the period *P* indicated in Table 2. (d) Finding chart for the target.

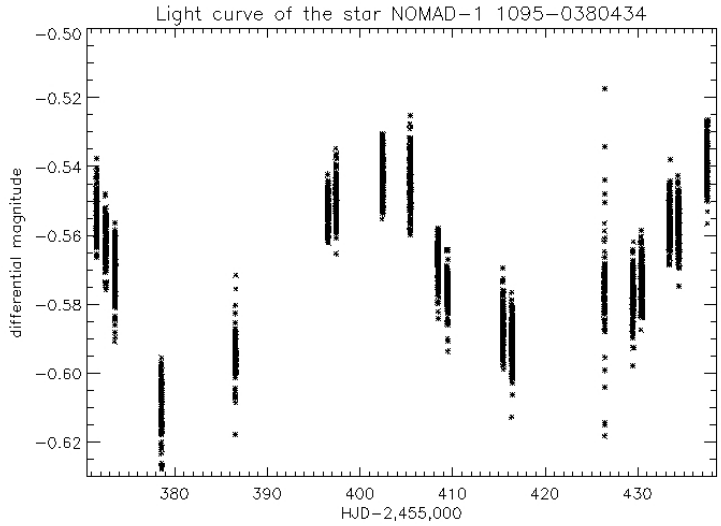

(a)

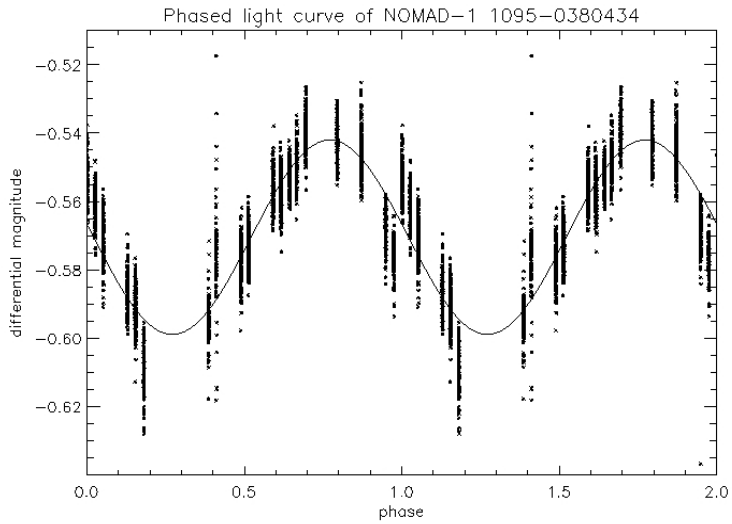

(b)

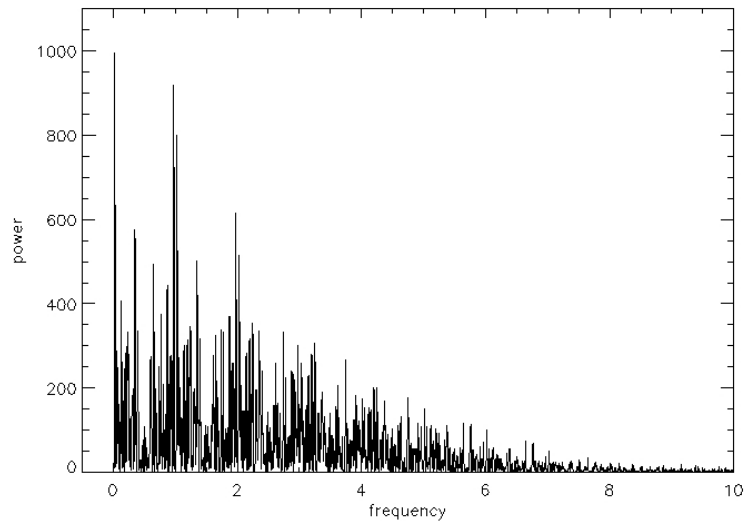

(c)

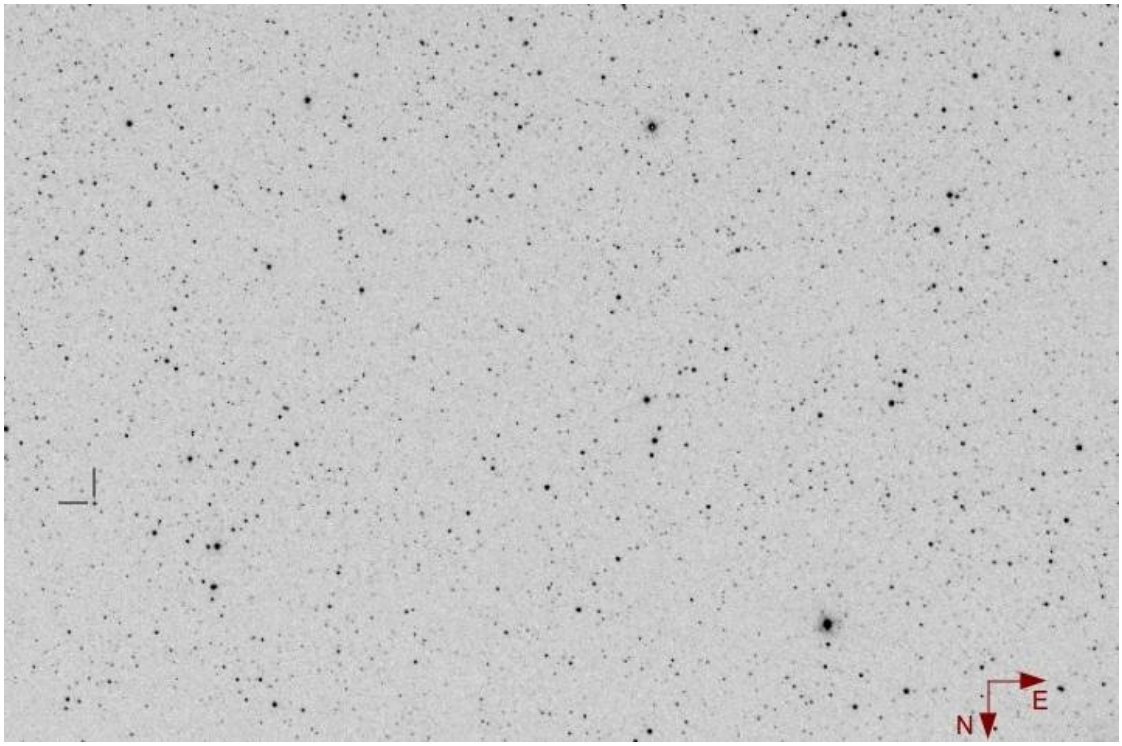

(d)

Figure 4 – (Up) Light curve of the star NOMAD-1 1093-0380200. This is probably a Mira or a SR pulsator. (Down)

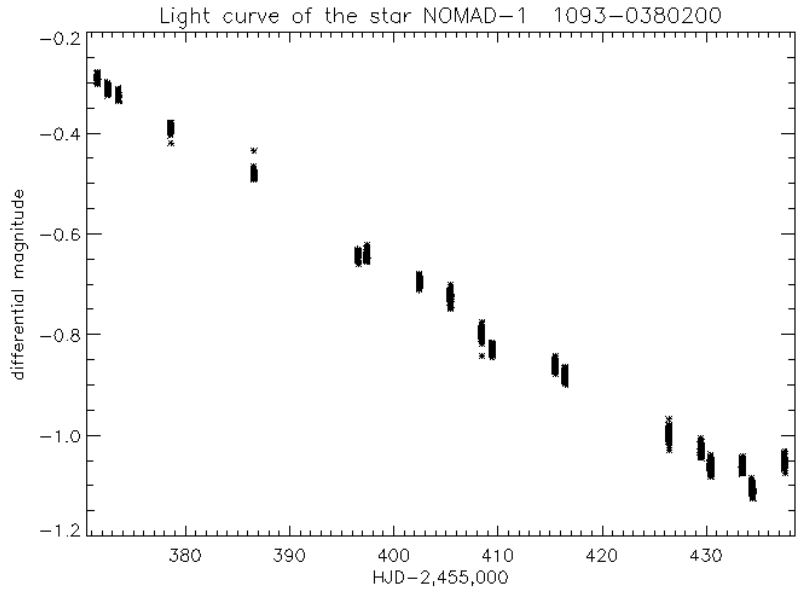

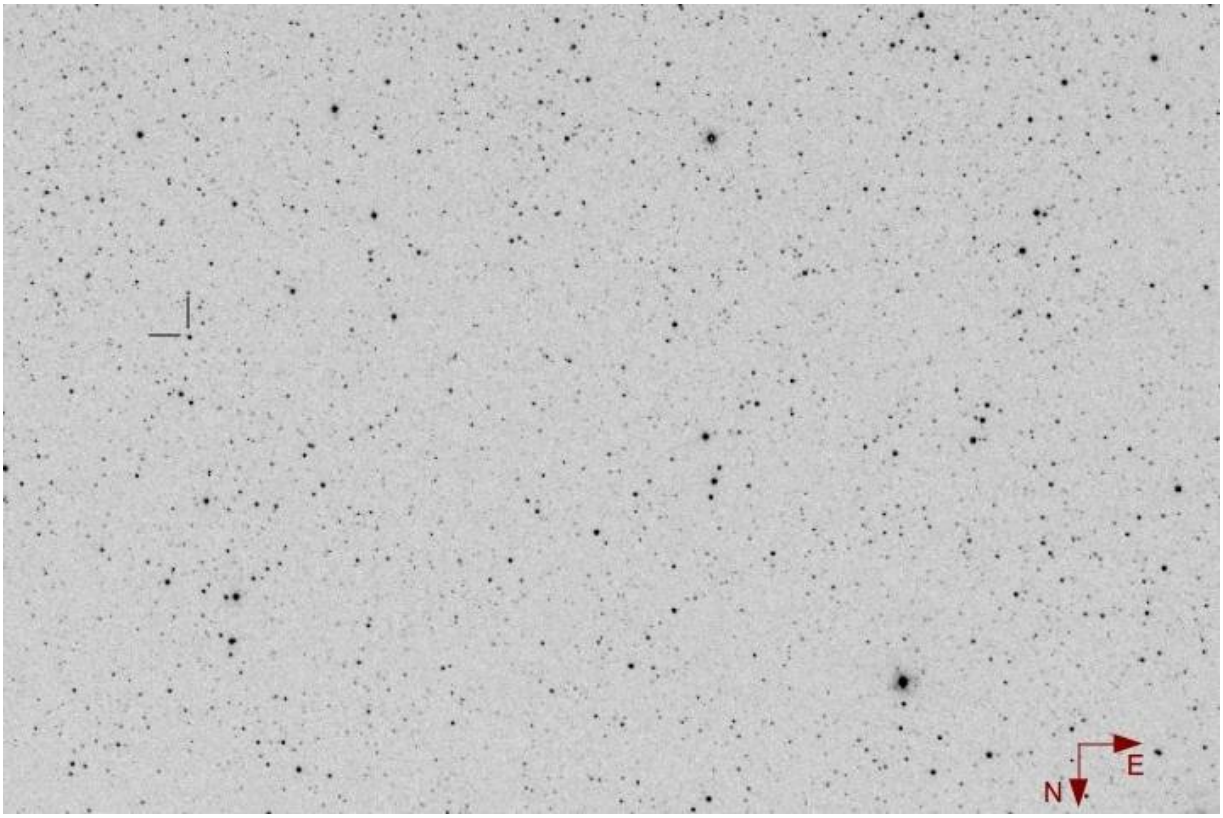

Figure 5 – (Up) Original light curve of the star NOMAD-1 1095-0380572. (Down) Finding chart for the target.

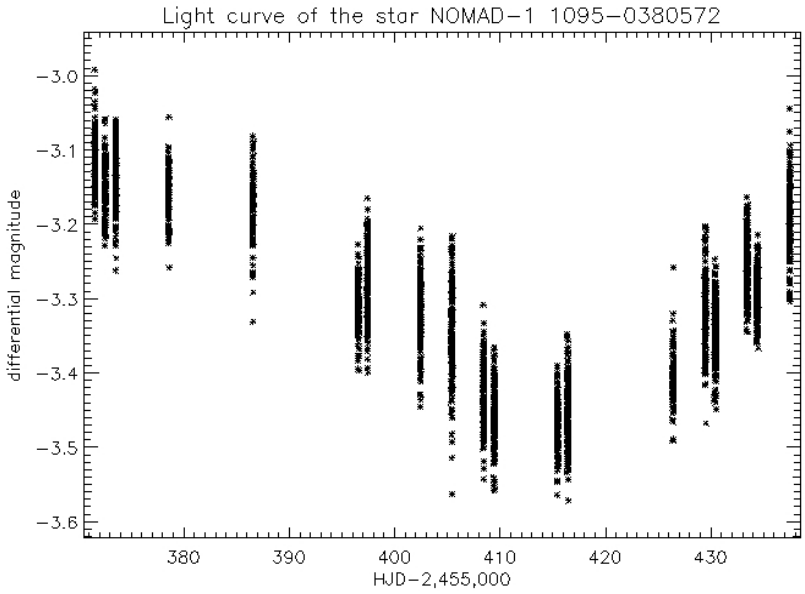

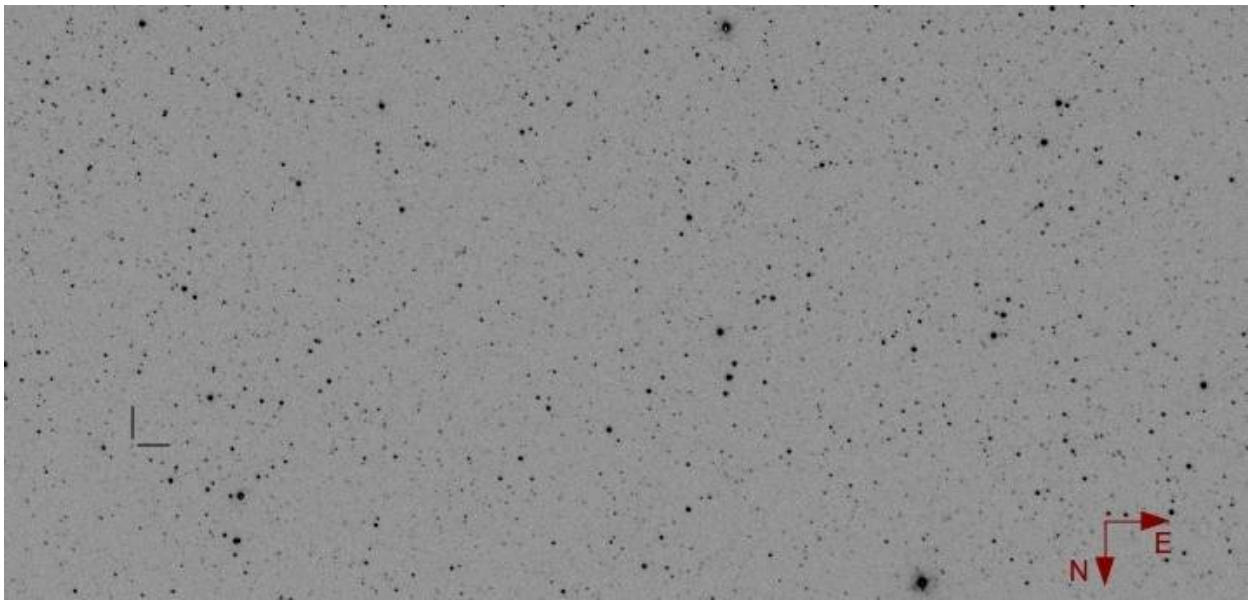

Figure 6 – (a) Original light curve of the star NOMAD-1 1095-0381014. (b) The phased light curve. Overplotted is the best fit sine curve. (c) The Lomb-Scargle periodogram. The peak frequency corresponds to the period *P* indicated in Table 2. (d) Finding chart for the target.

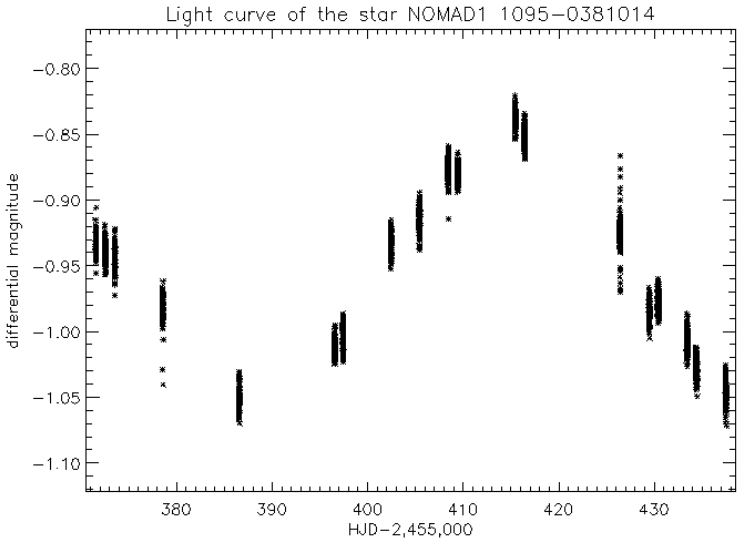

(a)

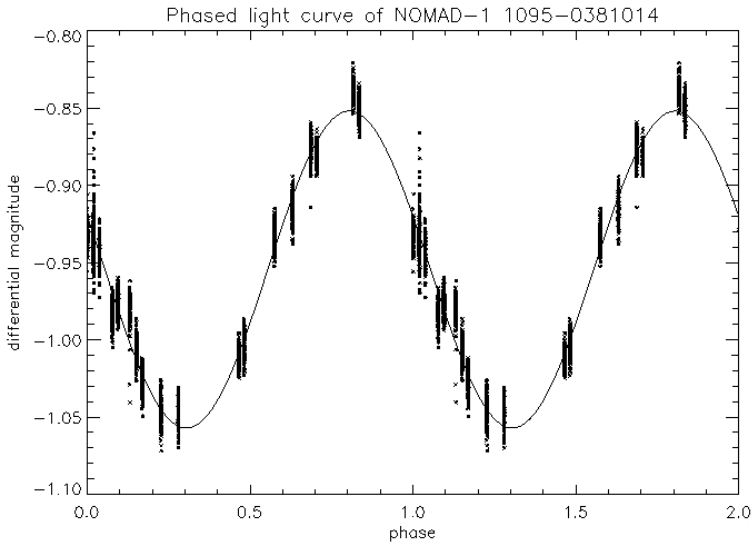

(b)

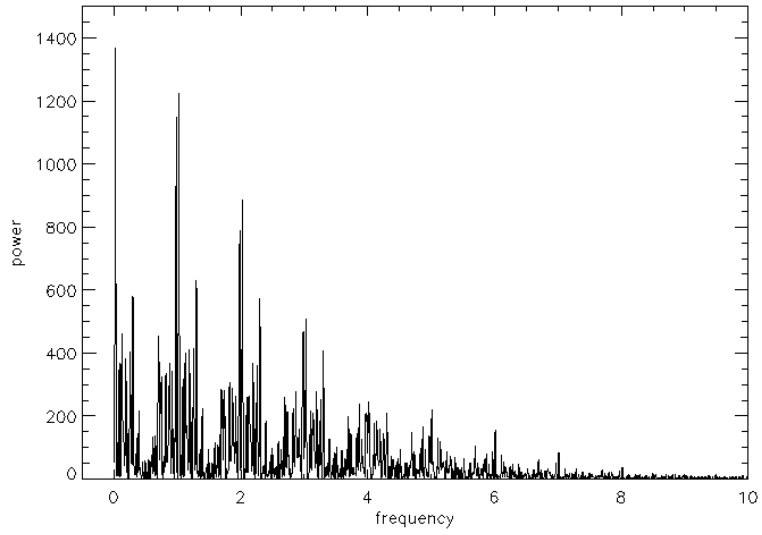

(c)

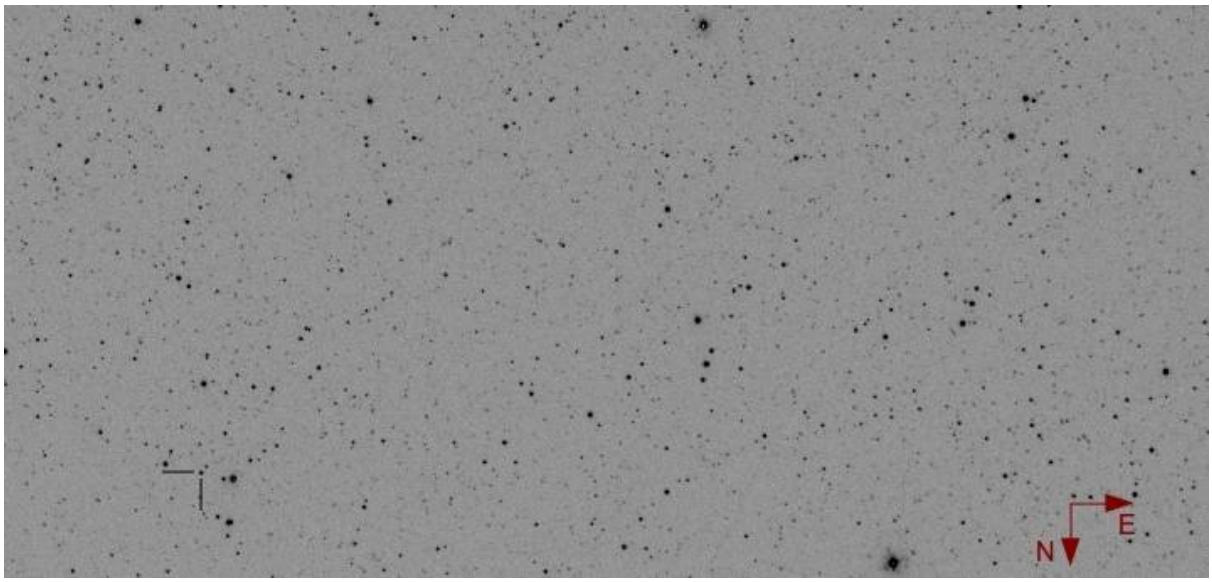

(d)

Figure 7 – (Up) Light curve of the star NOMAD-1 1095-0381250. This is probably a Mira or a SR pulsator. (Down) Finding chart for the target.

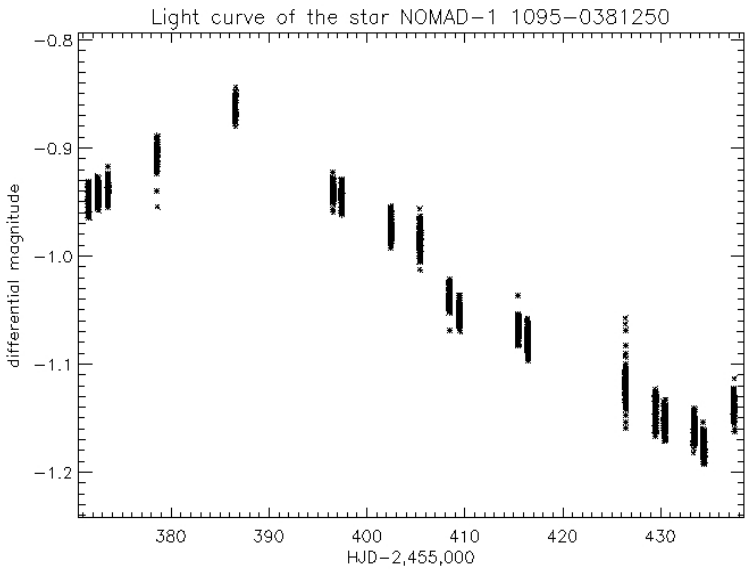

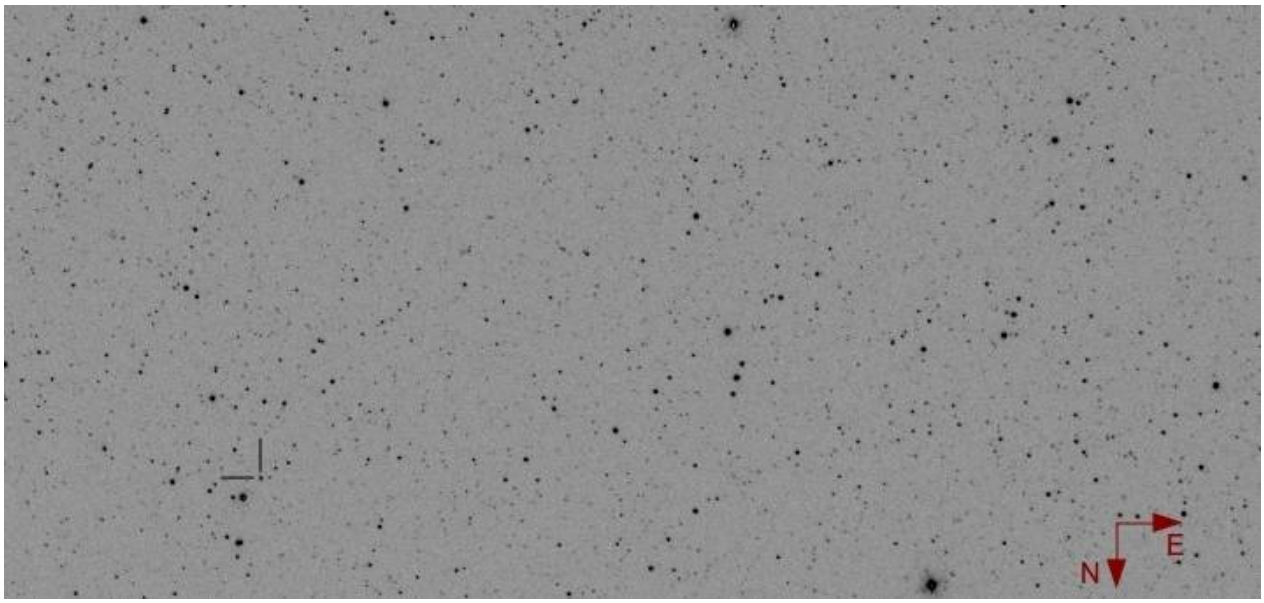

Figure 8 – (a) The original light curve of the star NOMAD-1 1090-0387525. (b) The phased light curve. Overplotted is the best fit sine curve. (c) The Lomb-Scargle periodogram. The peak frequency corresponds to the period *P* indicated in Table 2. (d) Finding chart for the target.

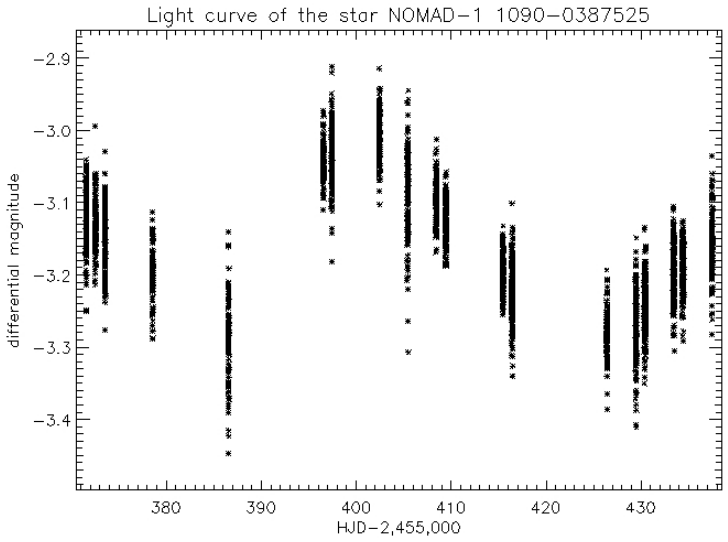

(a)

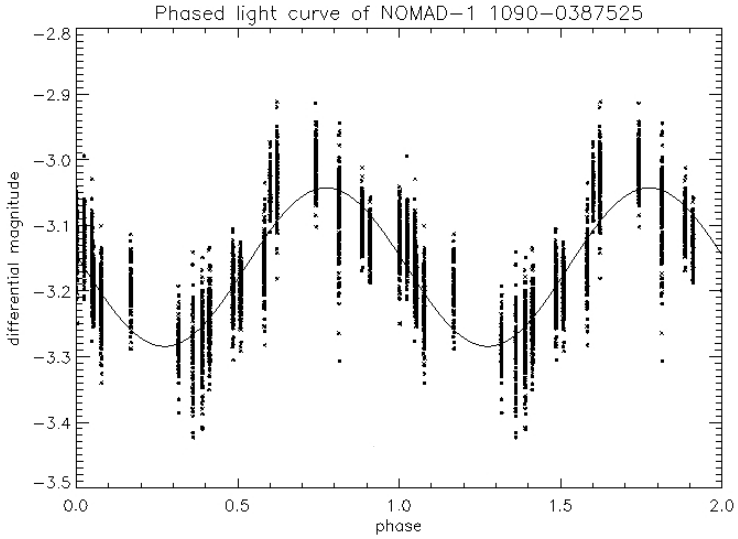

(b)

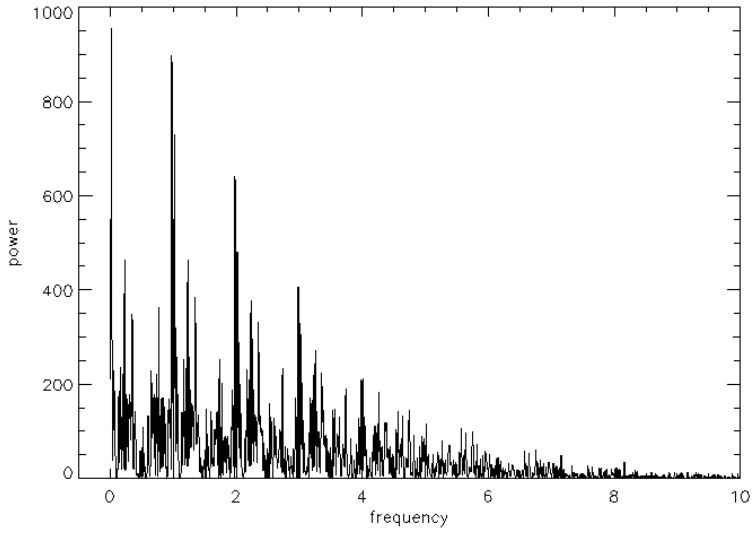

(c)

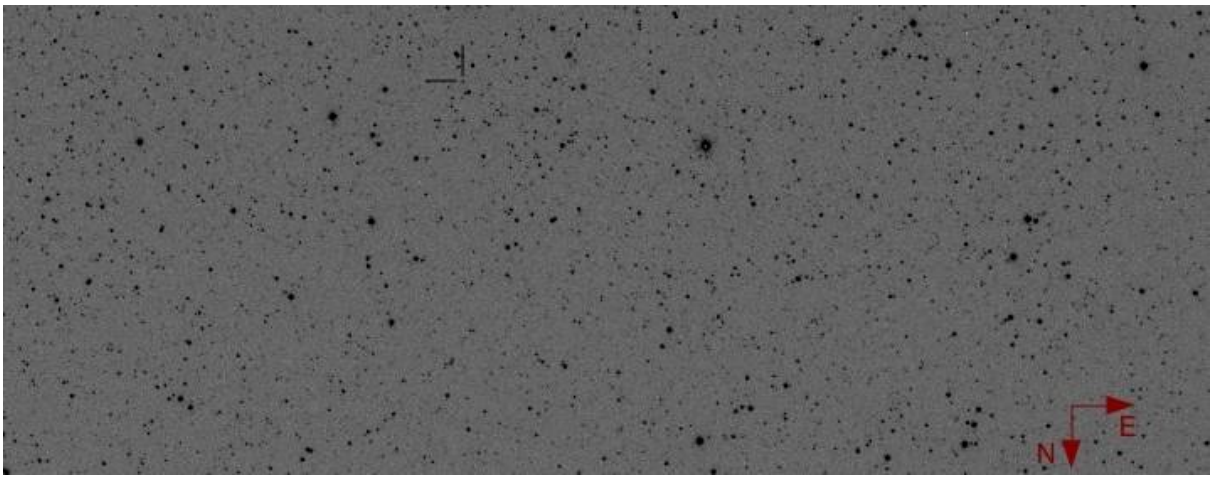

(d)

Figure 9 – Light curve of the star NOMAD-1 1093-0381534.

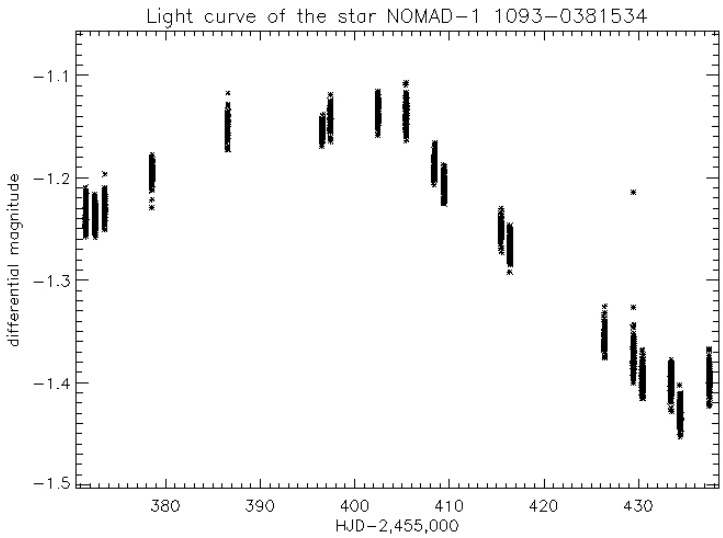

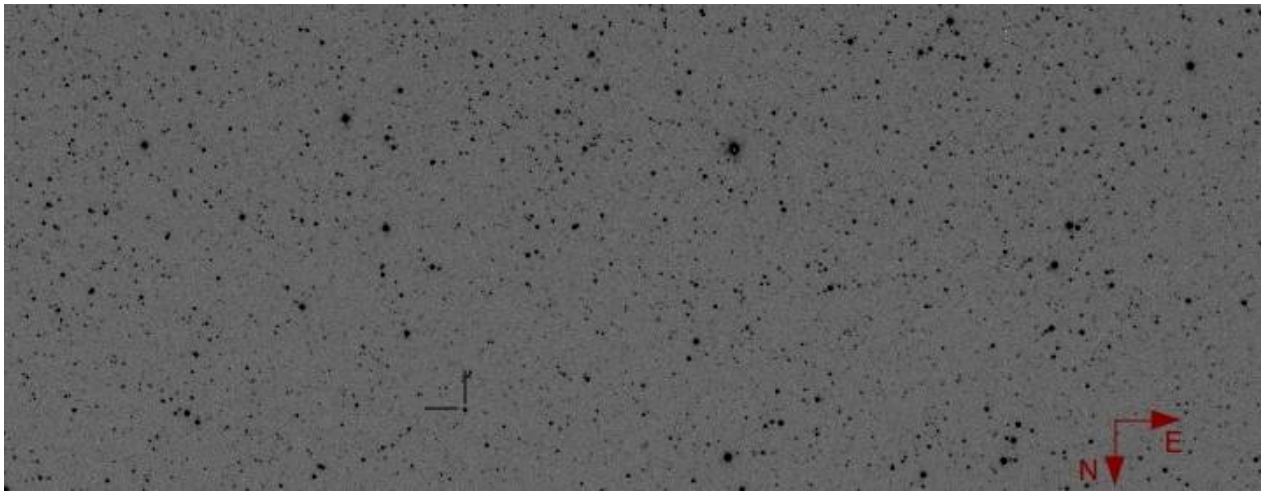

Figure 10 – (a) Original light curve of the star NOMAD-1 1095-0382124. (b) The phased light curve. Overplotted is the best fit sine curve. (c) The Lomb-Scargle periodogram. The peak frequency corresponds to the period *P* indicated in Table 2. (d) Finding chart for the target.

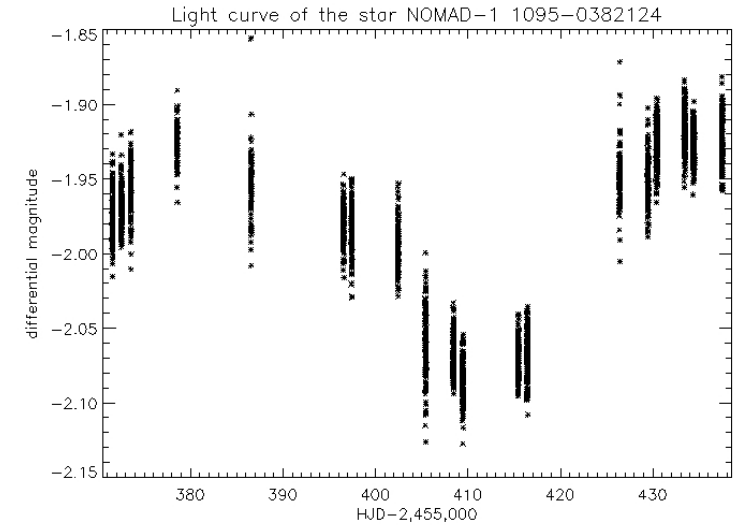

(a)

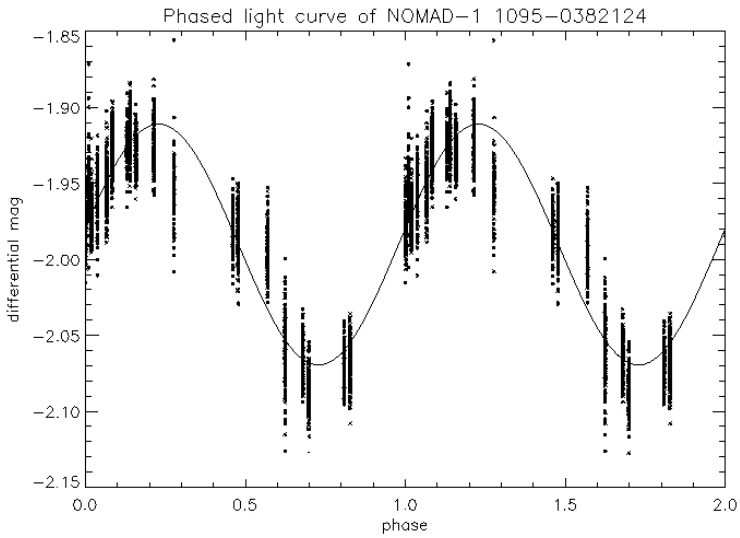

(b)

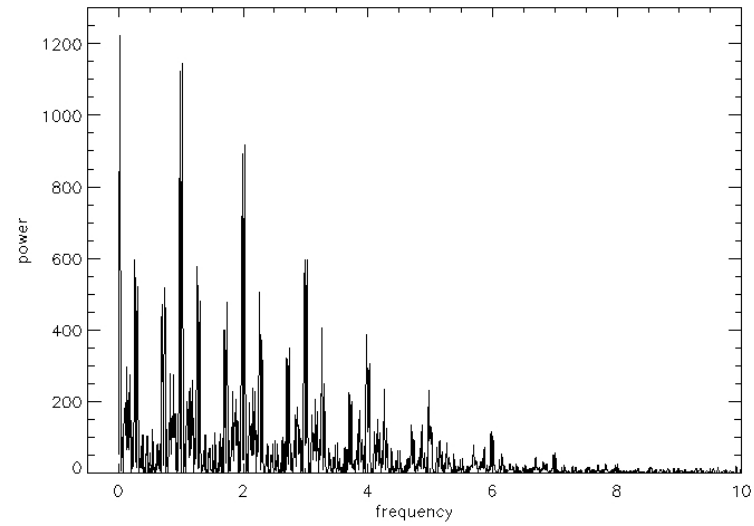

(c)

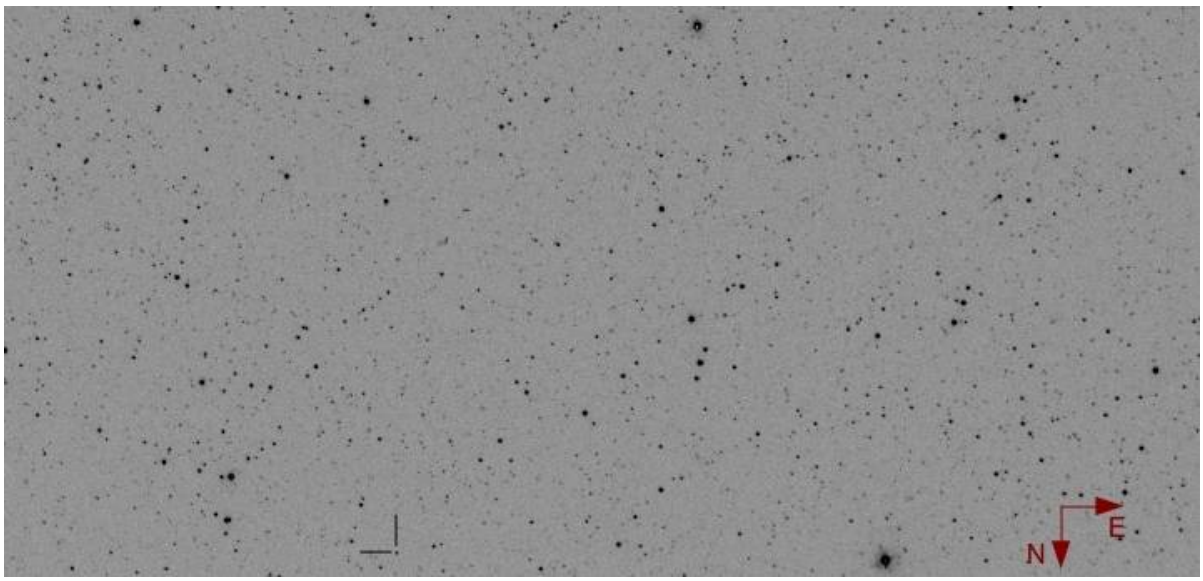

(d)

Figure 11 – (Up) Light curve of the star NOMAD-1 1090-0388621. (Down) Finding chart for the target

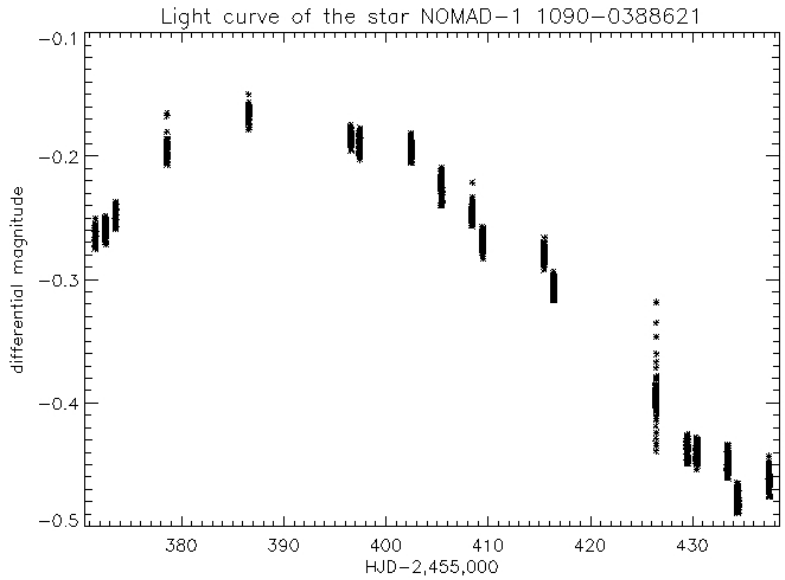

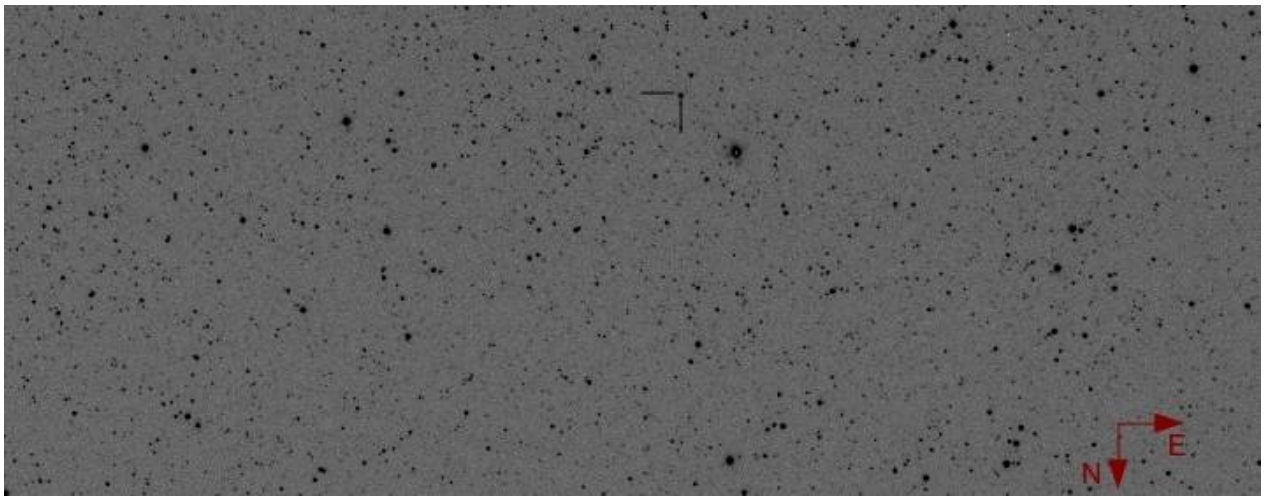

Figure 12 – (Up) Original light curve of the star NOMAD-1 1091-0387997. (Down) Finding chart for the target.

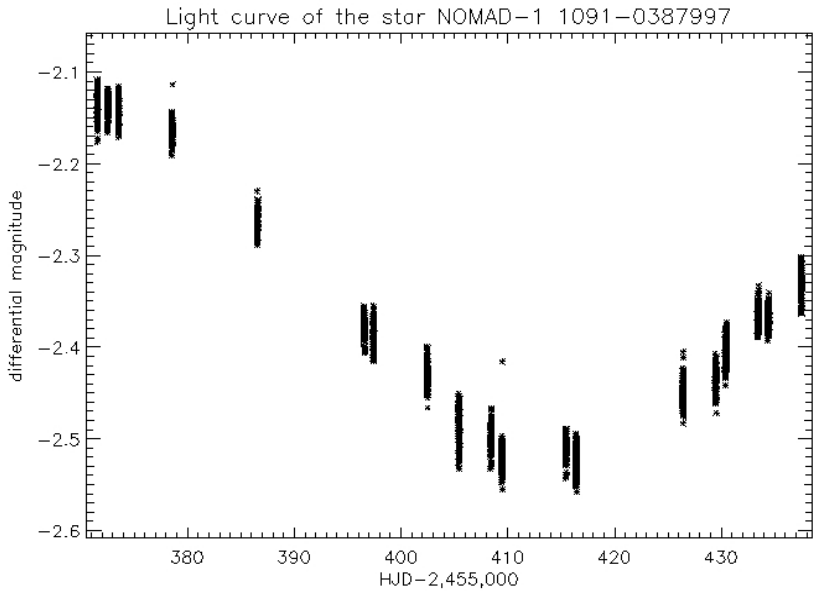

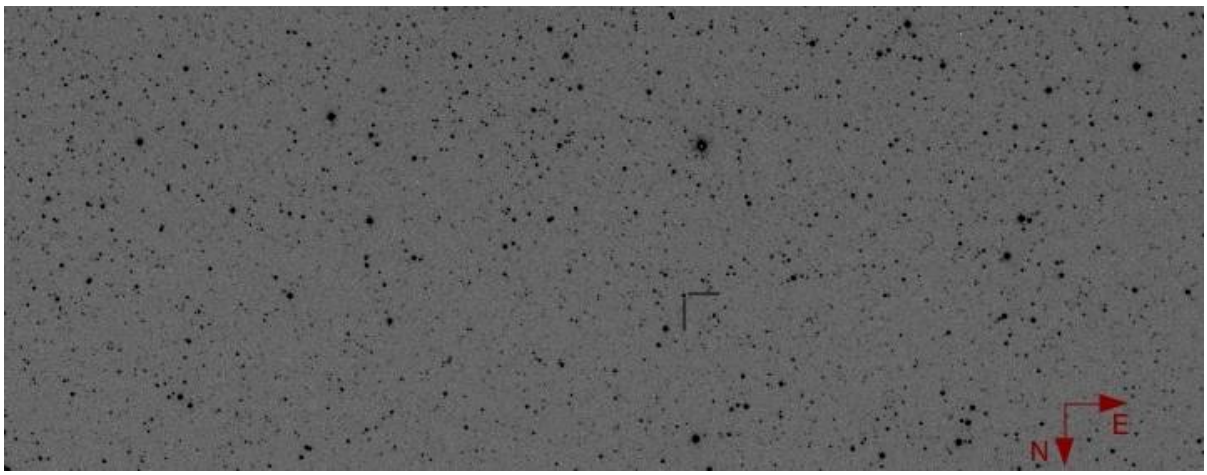

Figure 13 – (a) Original light curve of the star NOMAD-1 1093-0382699. (b) The phased light curve. Overplotted is the best fit sine curve. (c) The Lomb-Scargle periodogram. The peak frequency corresponds to the period *P* indicated in Table 2. (d) Finding chart for the target.

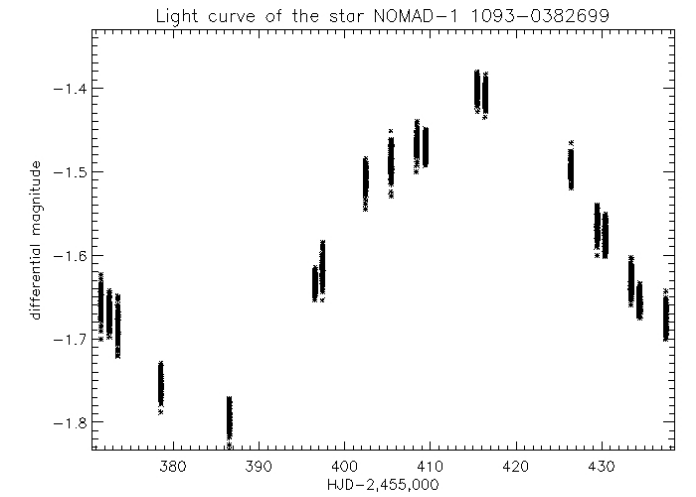

(a)

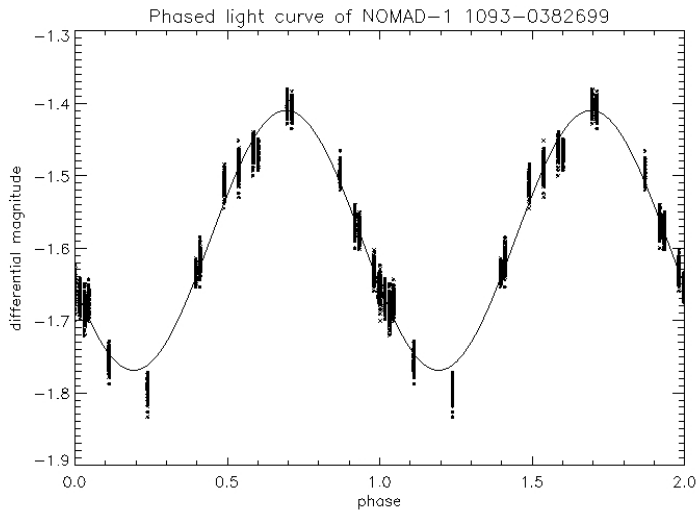

(b)

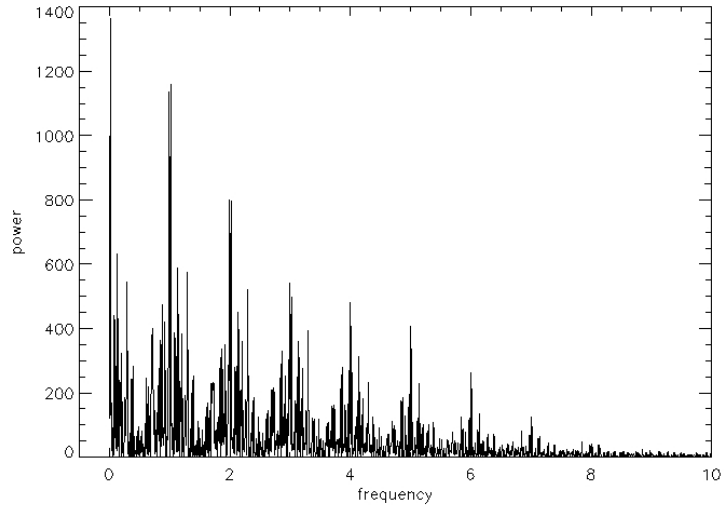

(c)

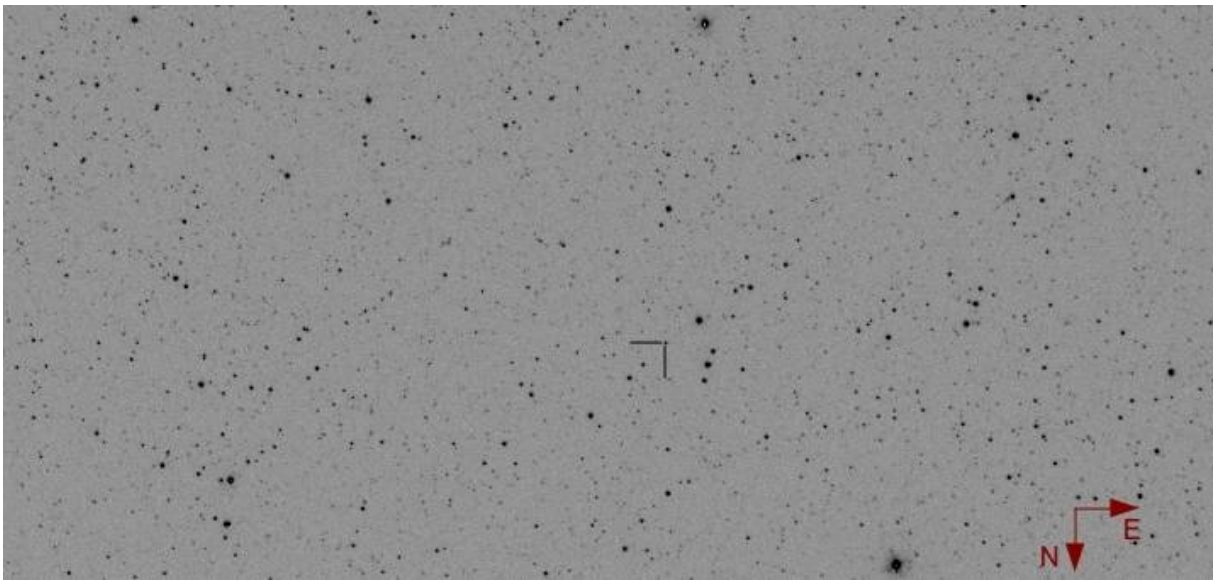

(d)

Figure 14 – (Up) Light curve of the star NOMAD-1 1090-0389865. (Down) Finding chart for the target.

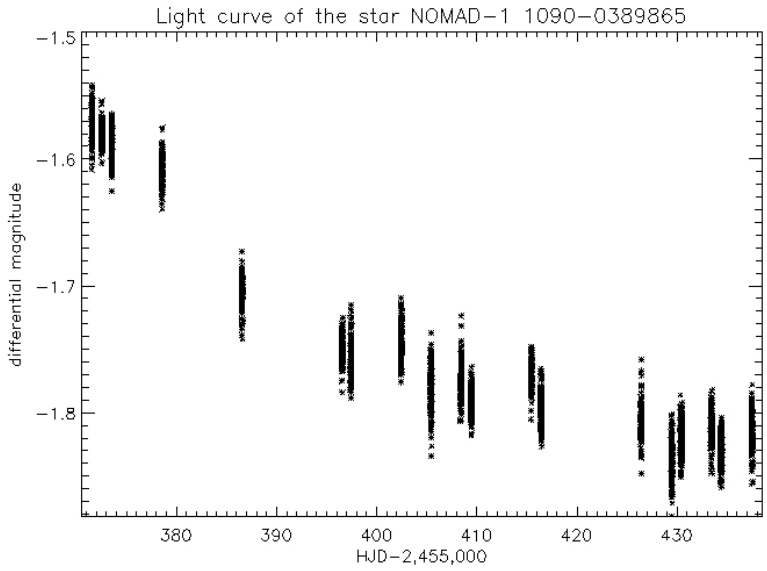

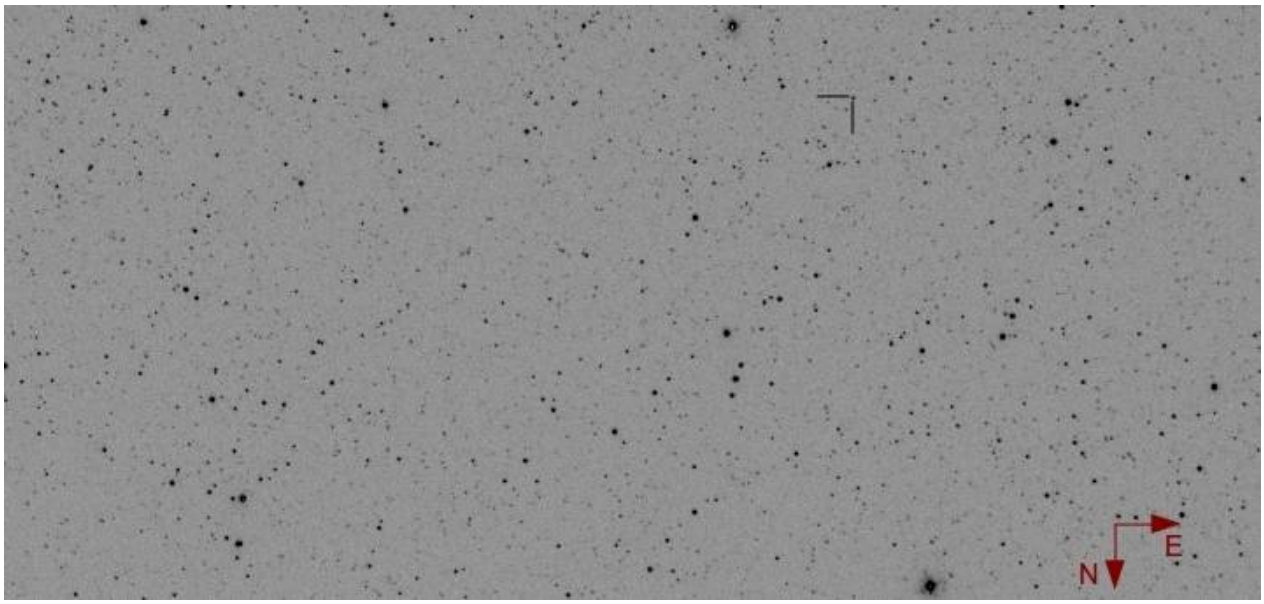

Figure 15 – (a) Original light curve of the star NOMAD-1 1094-0383234. (b) The phased light curve. Overplotted is the best fit sine curve. (c) The Lomb-Scargle periodogram. The peak frequency corresponds to the period *P* indicated in Table 2. (d) Finding chart for the target.

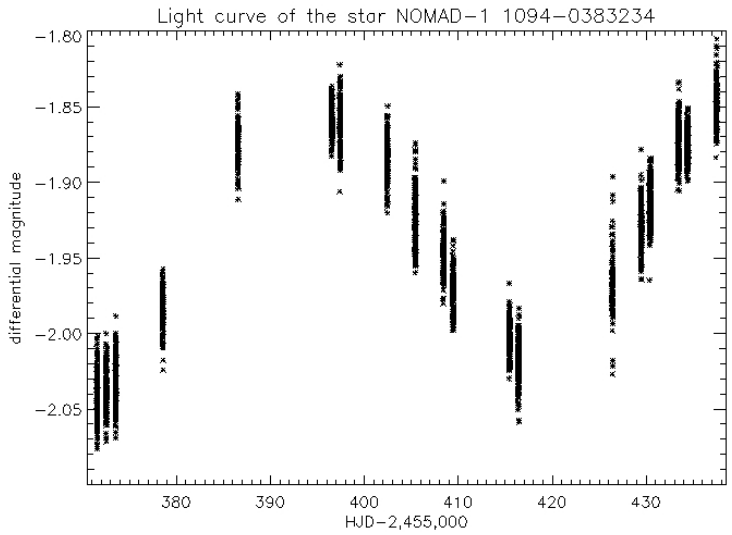

(a)

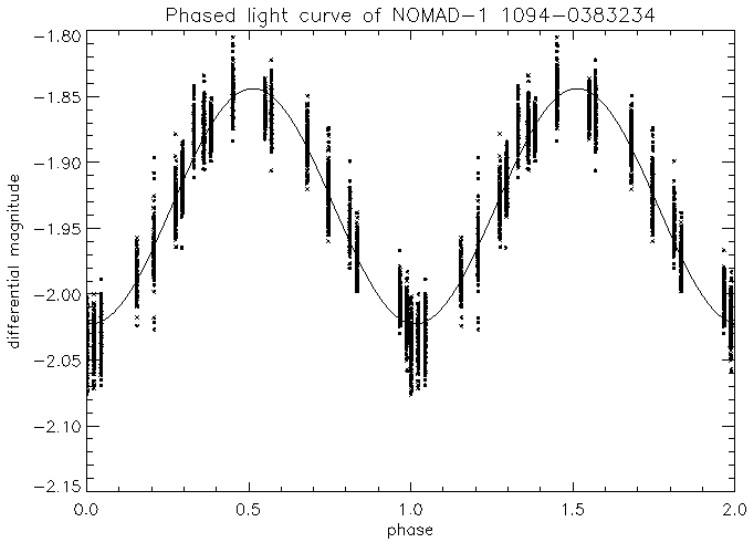

(b)

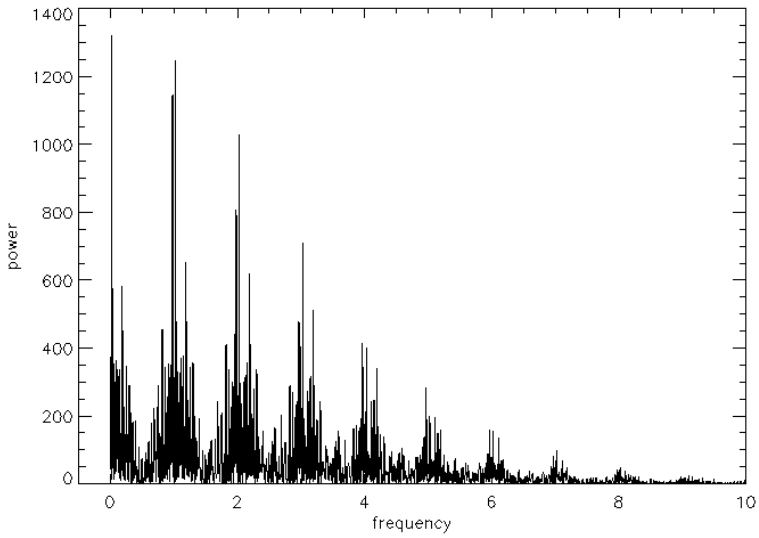

(c)

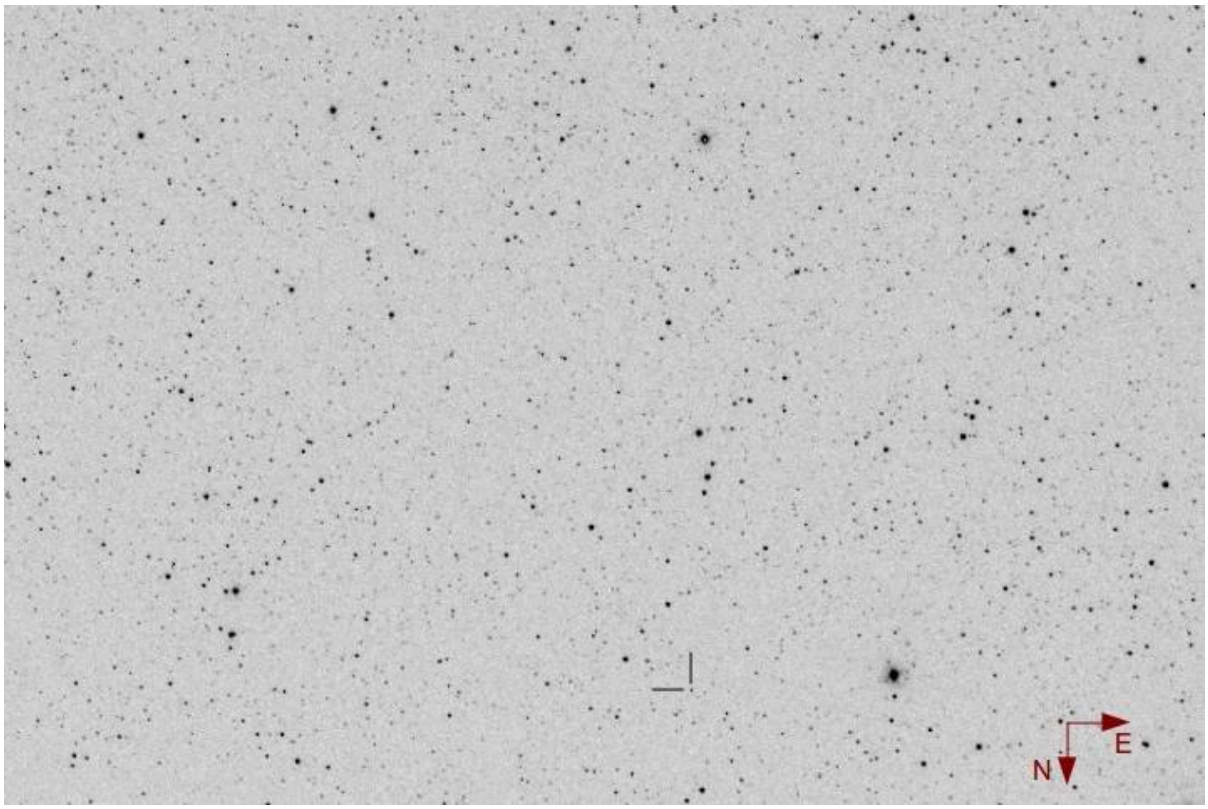

(d)

Figure 16 – (Up) Light curve of the star NOMAD-1 1092-0387428. This is probably a Mira or a SR pulsator. (Down) Finding chart for the target.

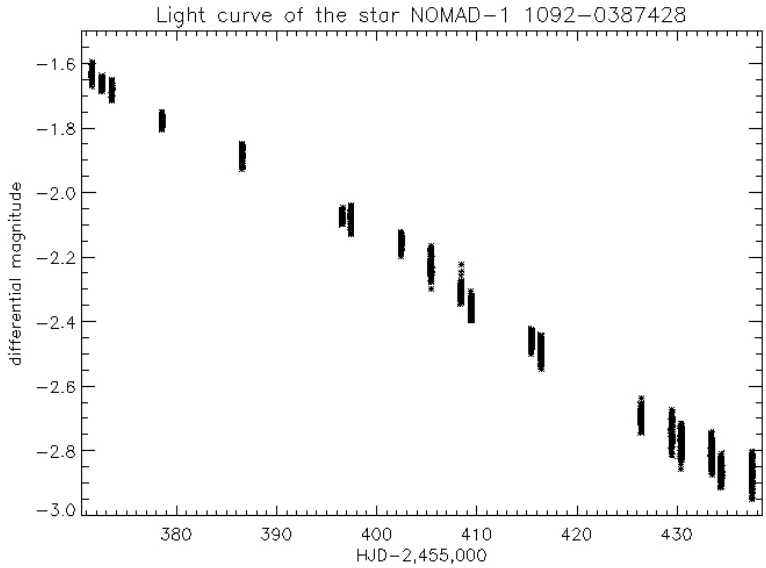

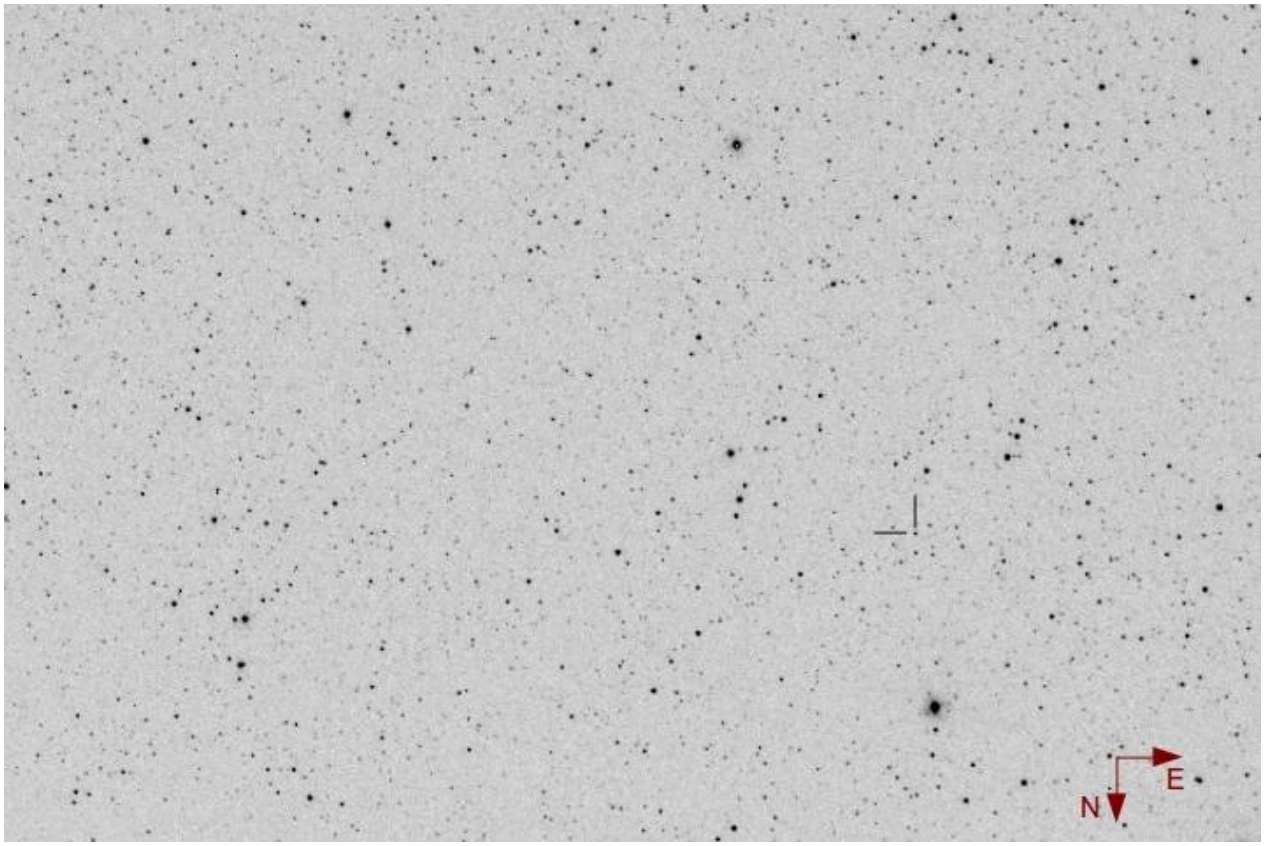

Figure 17 – (a) Original light curve of the star NOMAD-1 1091-0389915. (b) The phased light curve. Overplotted is the best fit sine curve. (c) The Lomb-Scargle periodogram. The peak frequency corresponds to the period *P* indicated in Table 2. (d) Finding chart for the target.

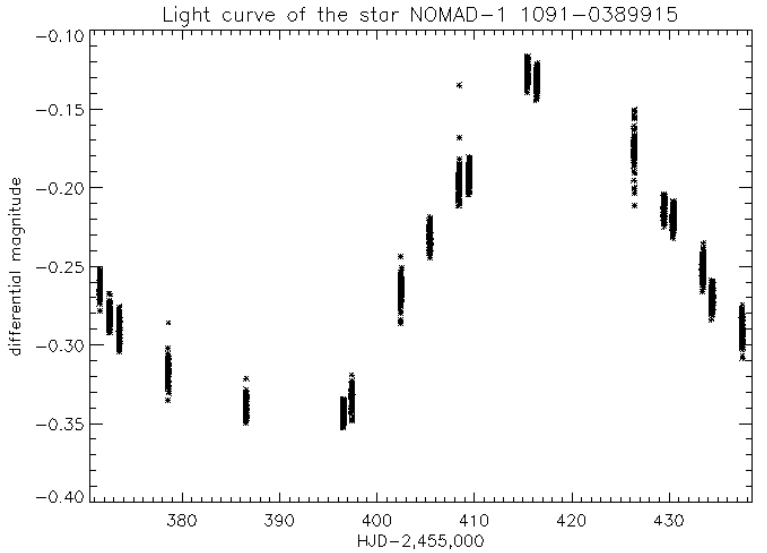

(a)

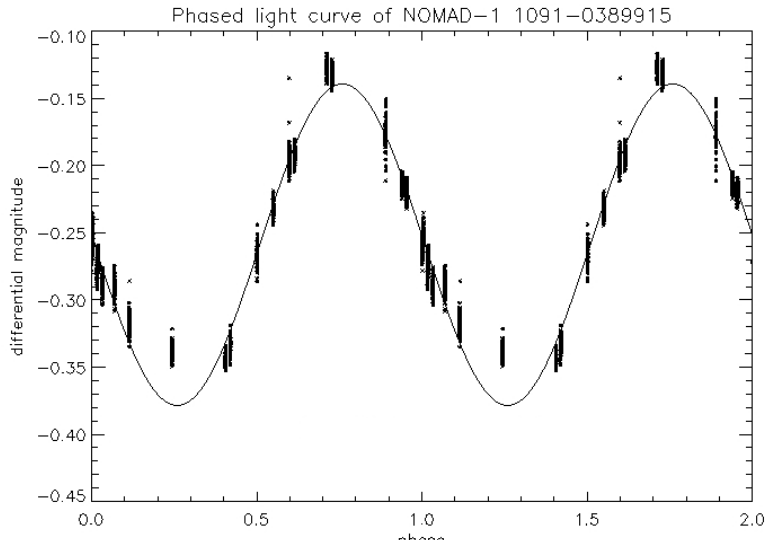

(b)

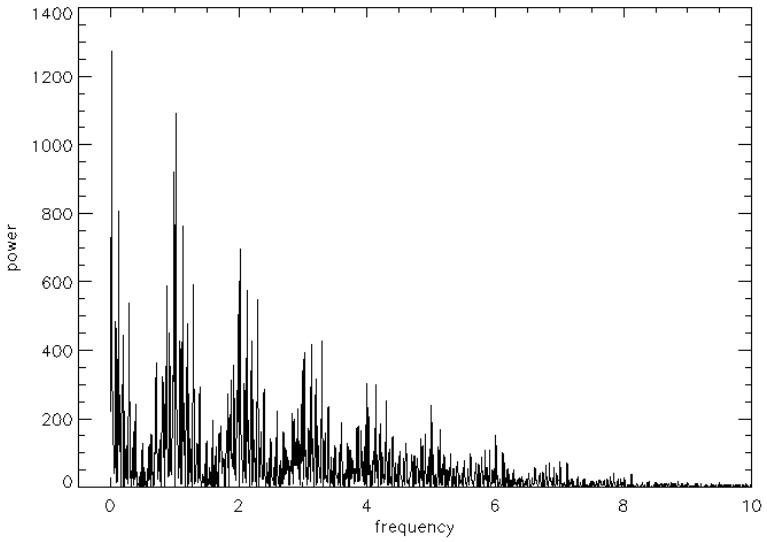

(c)

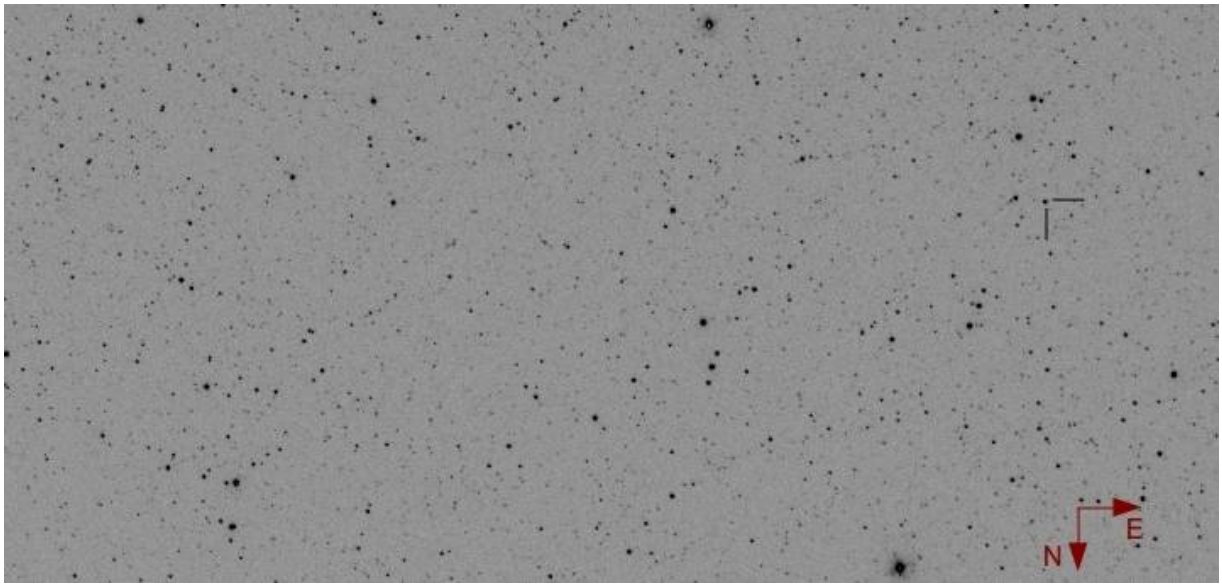

(d)

Figure 18 – (Up) Light curve of the star NOMAD-1 1092-0388944. (Down) Finding chart for the target.

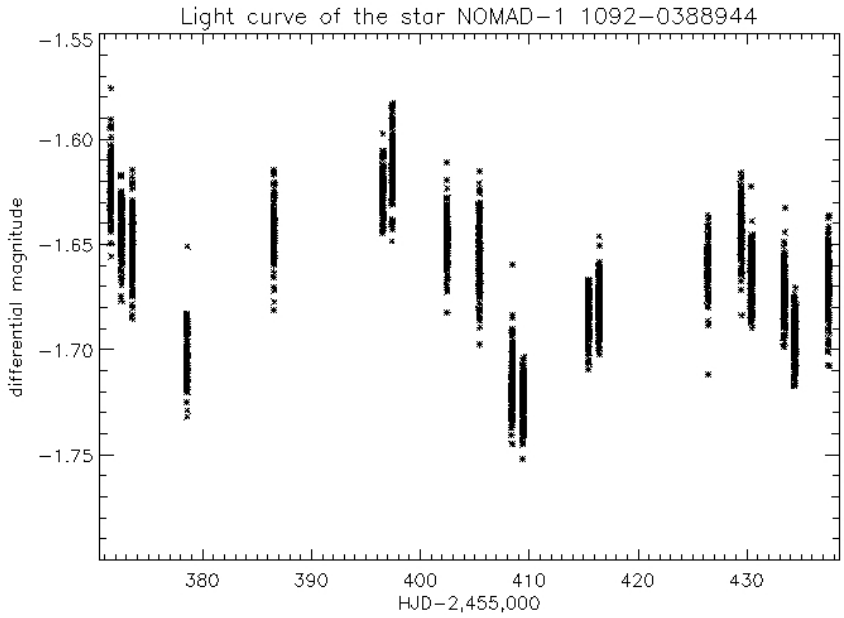

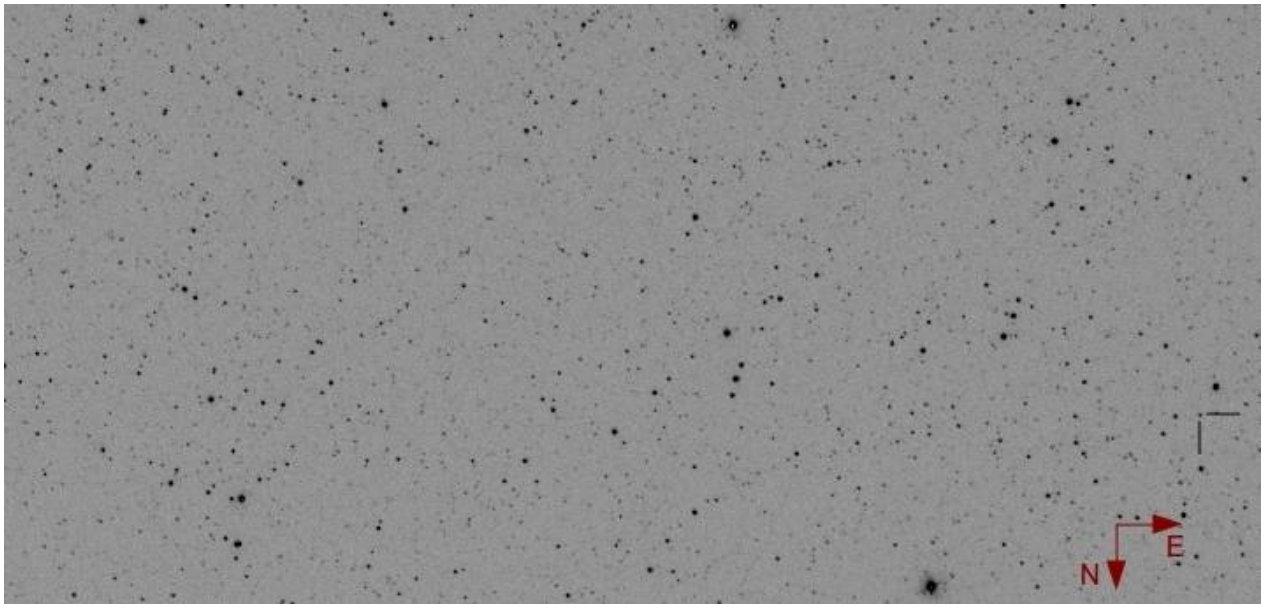

Figure 19 – (a) Light curve of the pulsating star NOMAD-1 1077-0767537 phased according the frequency F1=7.45248377 cycle/day. (b) Periodogram showing the peak corresponding to F1. (c) Residuals O-C phased according the frequency F2=4.52912947 cycle/day, showing that the residuals contain a significant periodicity. (d) Periodogram related to the Fourier analysis of the residuals, showing the peak corresponding to F2. (e) Finding chart for the target.

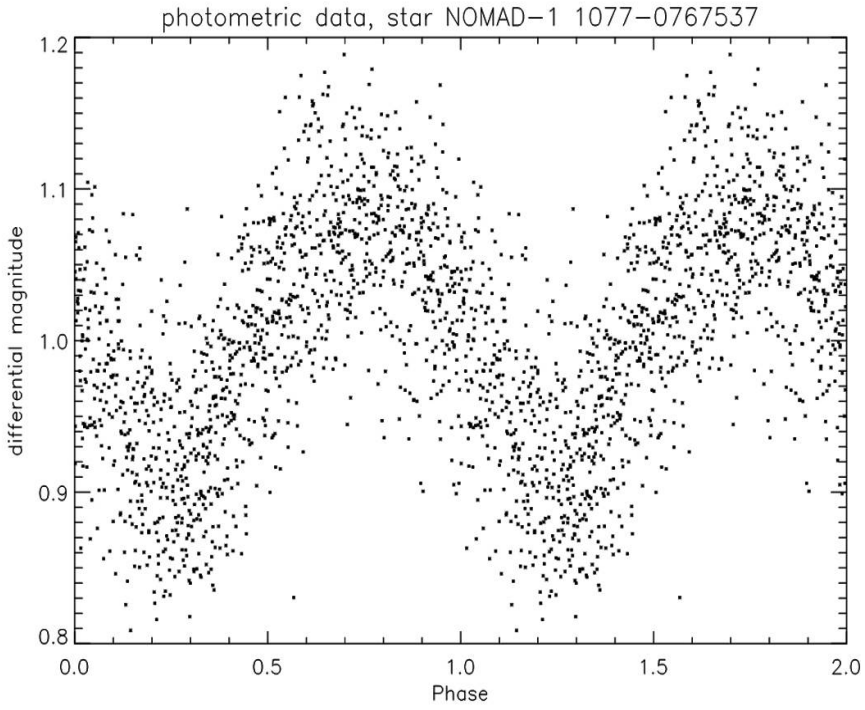

(a)

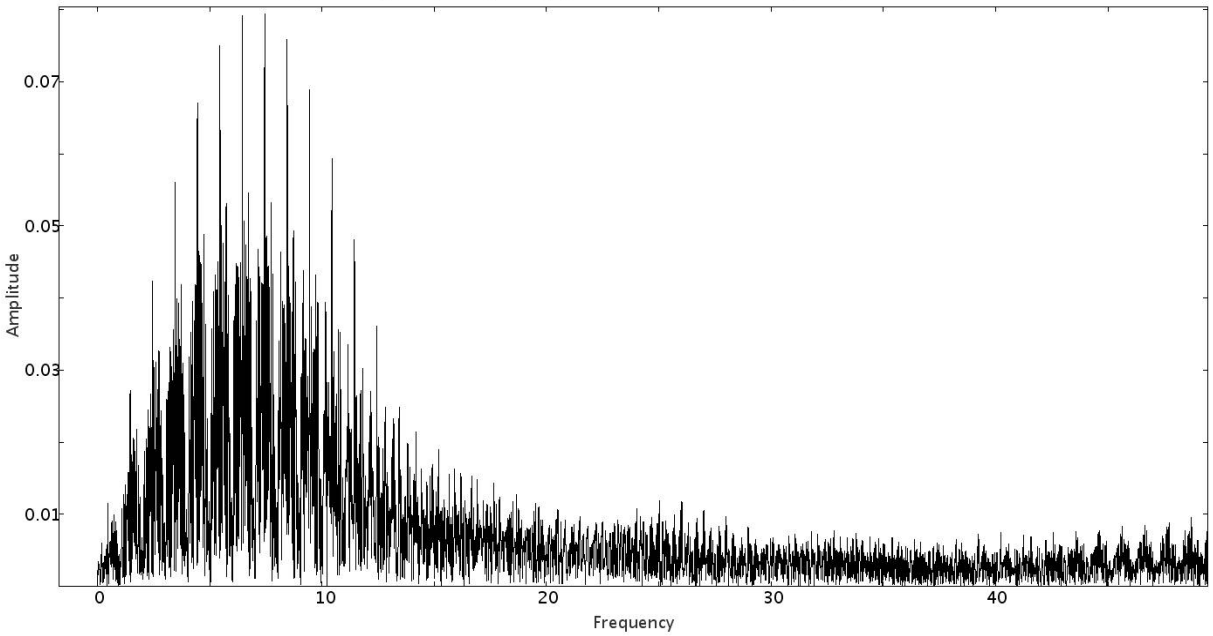

(b)

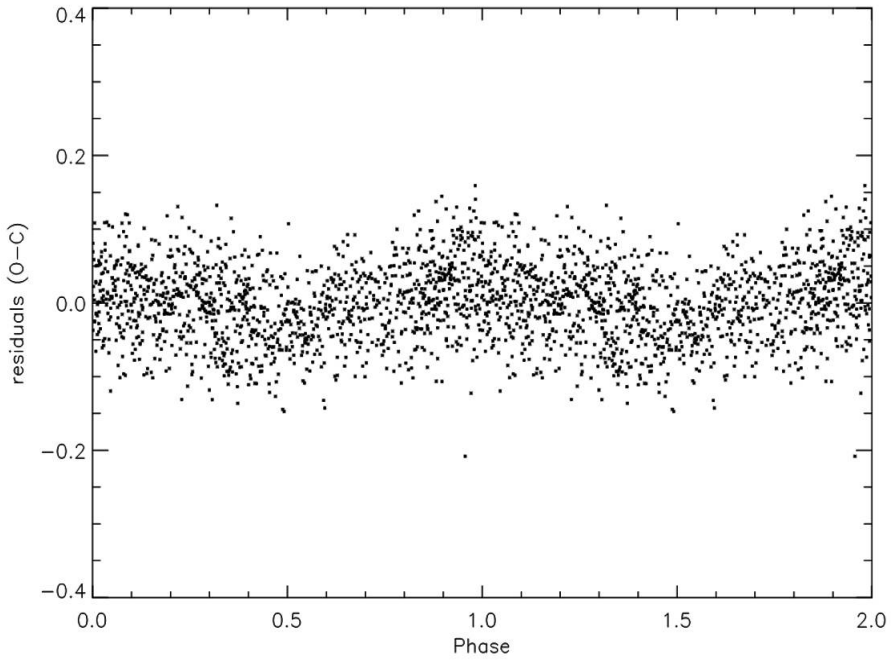
0.4
0.2
0.0
−0.2
−0.4
residuals (O−C)
0.0
0.5
1.0
1.5
2.0
Phase

(c)

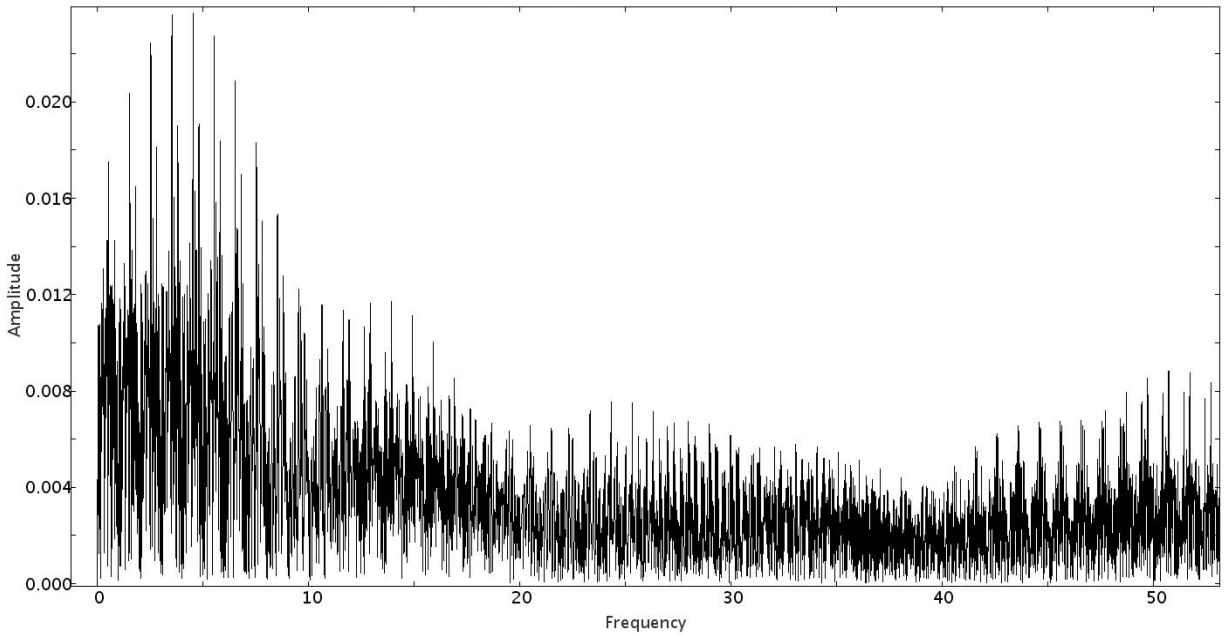
0.020
0.016
0.012
0.008
0.004
0.000
Amplitude
0
10
20
30
40
50
Frequency

(d)

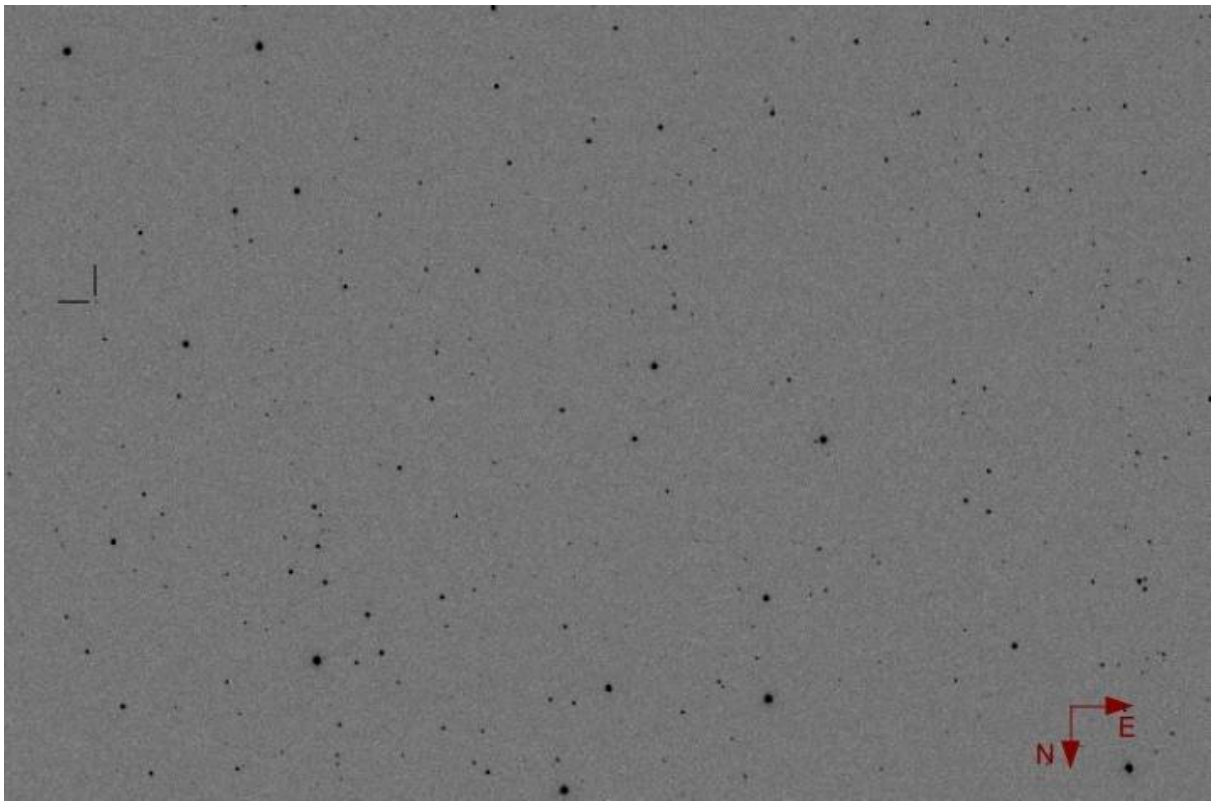

(e)

Figure 20 – (Up) Folded light curve of the object NOMAD-1 1617-0165649. (Down) Finding chart for the target.
The object can be classified as a W UMa eclipsing binary system. Data correspond to 37 nights of observations and are averaged in 200 bins.

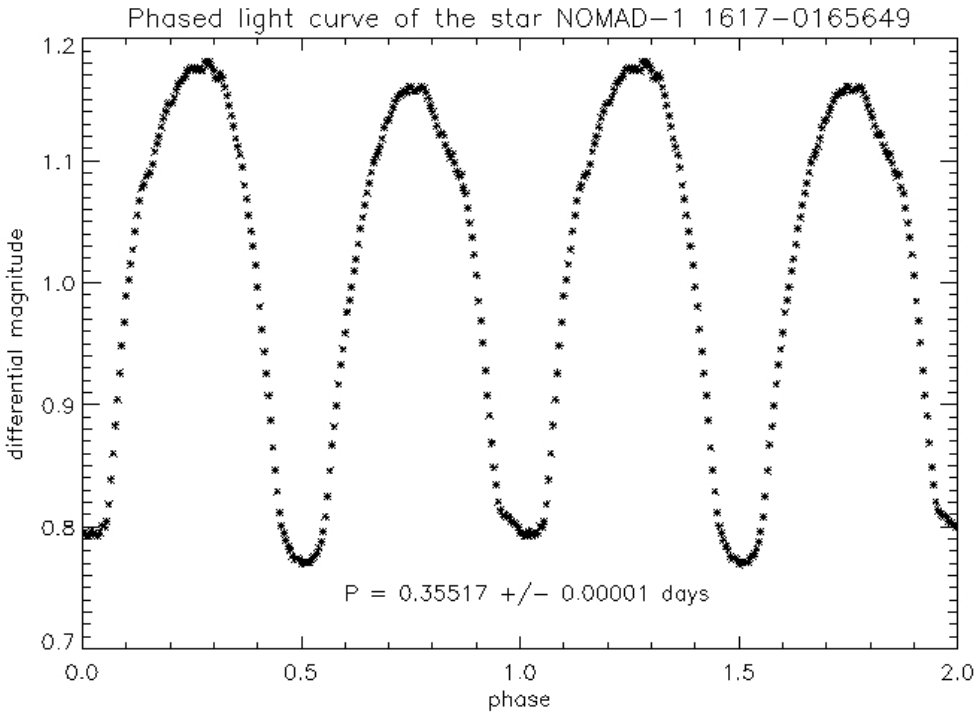

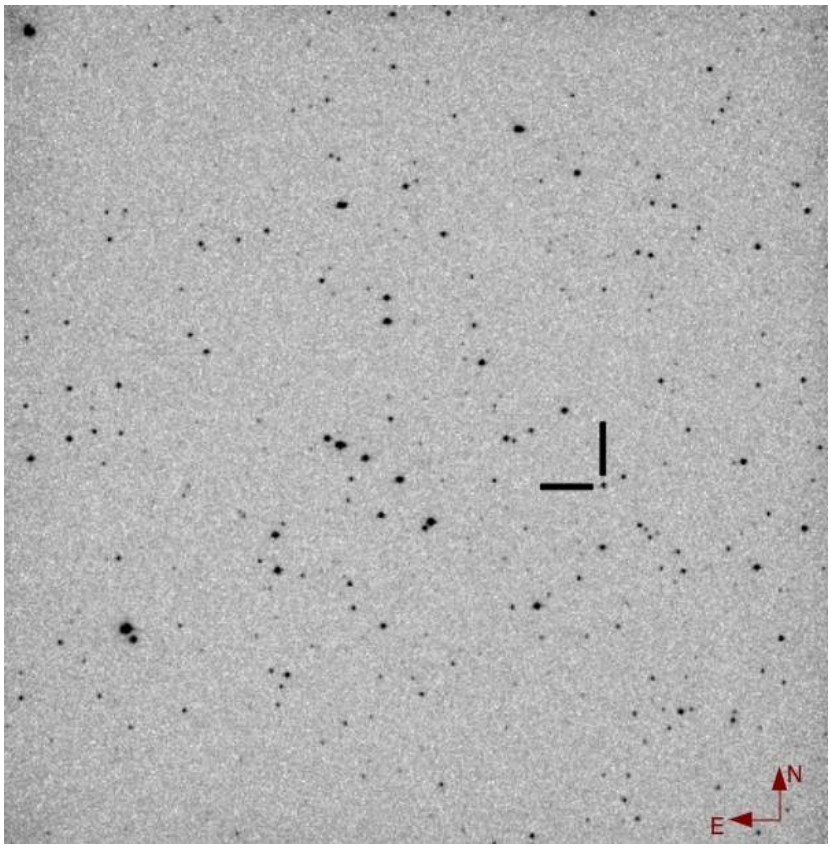

Figure 21 – Single-night light curves of the object NOMAD-1 1617-0165649. Changes from epoch to epoch in the shape of the minima is clearly evident, as for asymmetries in the parts corresponding to the maxima (this explain the global asymmetries present in the folded light curve of Fig. 20). This can be due to the presence of dark spots on the surfaces of both the system components. The epoch of observation is indicated at the top of each plot.

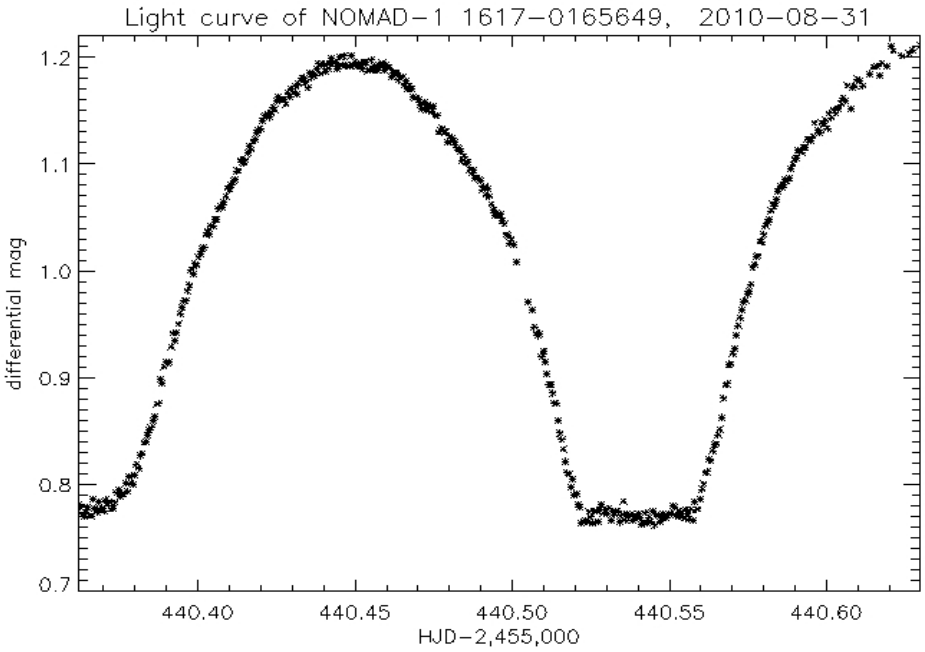

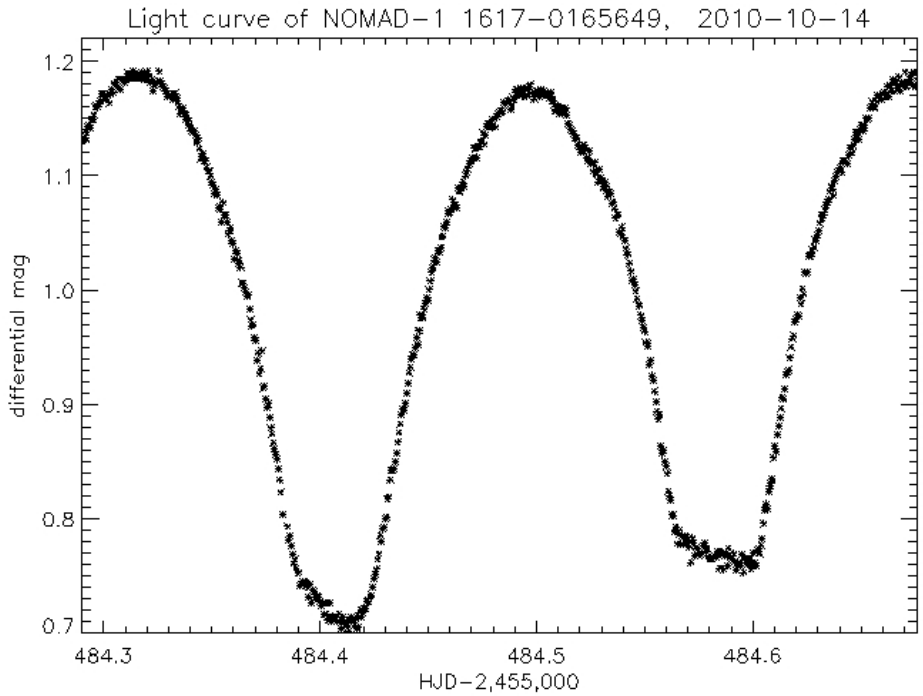

(Fig. 21 continued)

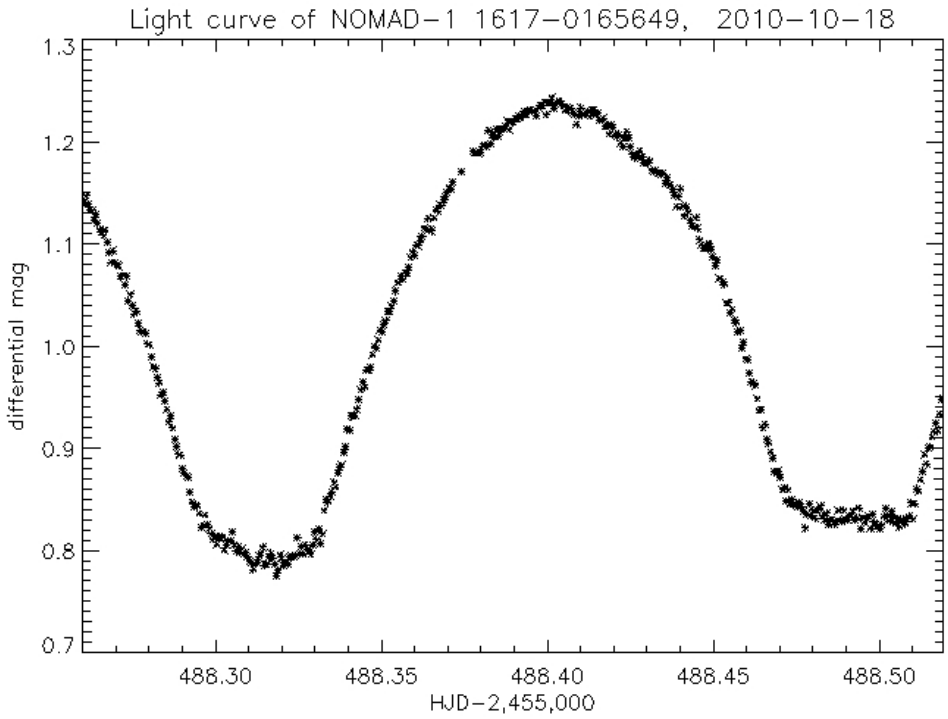

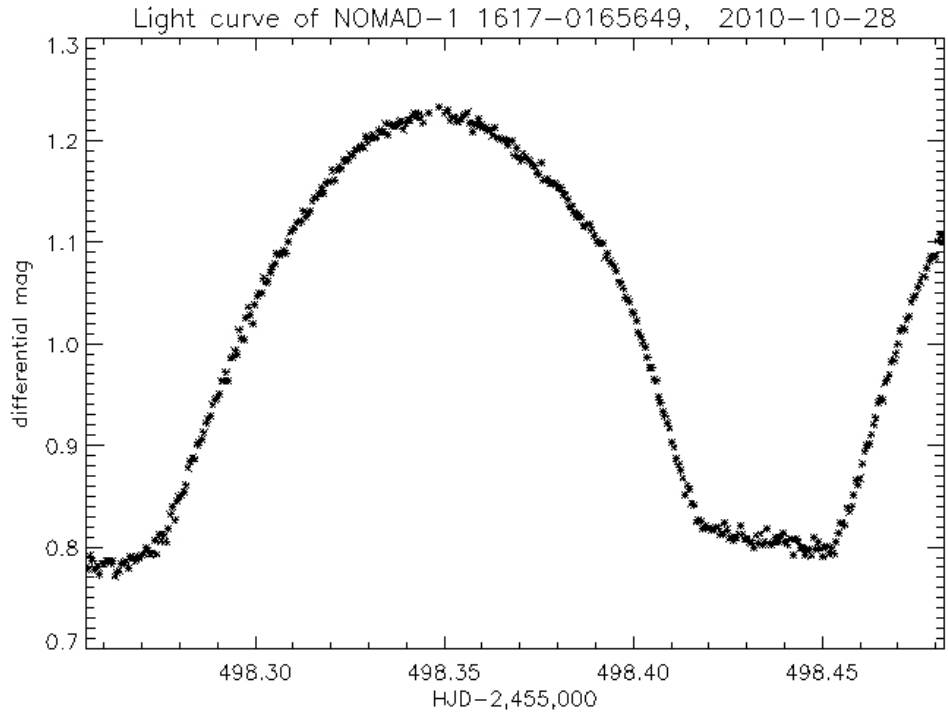

Figure 22 – (a) Folded light curve of the star NOMAD-1 1616-0162705 with the best fit sine curve superposed. (b) The periodogram showing the peak corresponding to the folding period P=0.10073 days. (c) Finding chart for the target.
The star may be classified as a Delta Scuti pulsating variable.

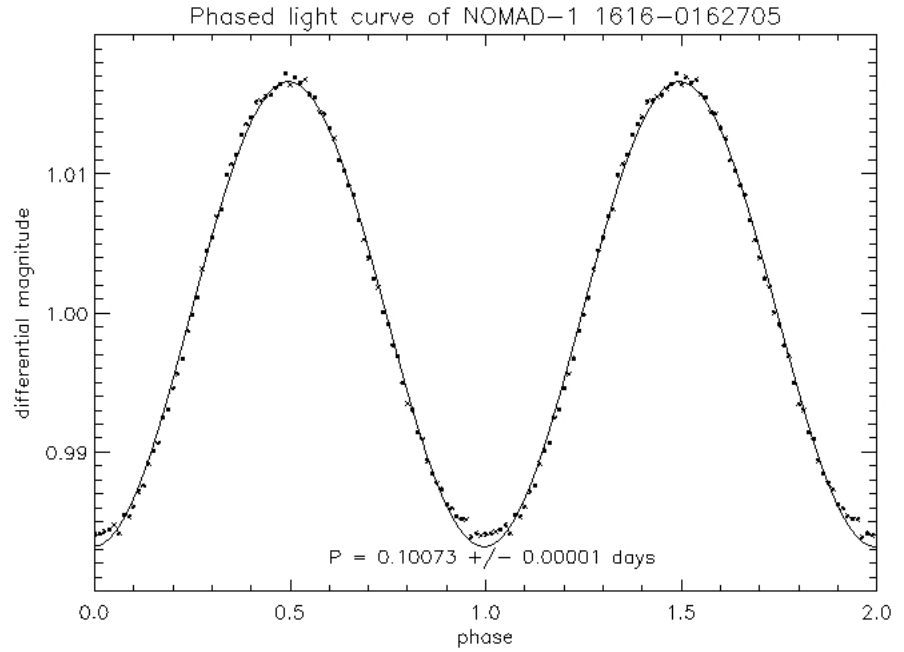

(a)

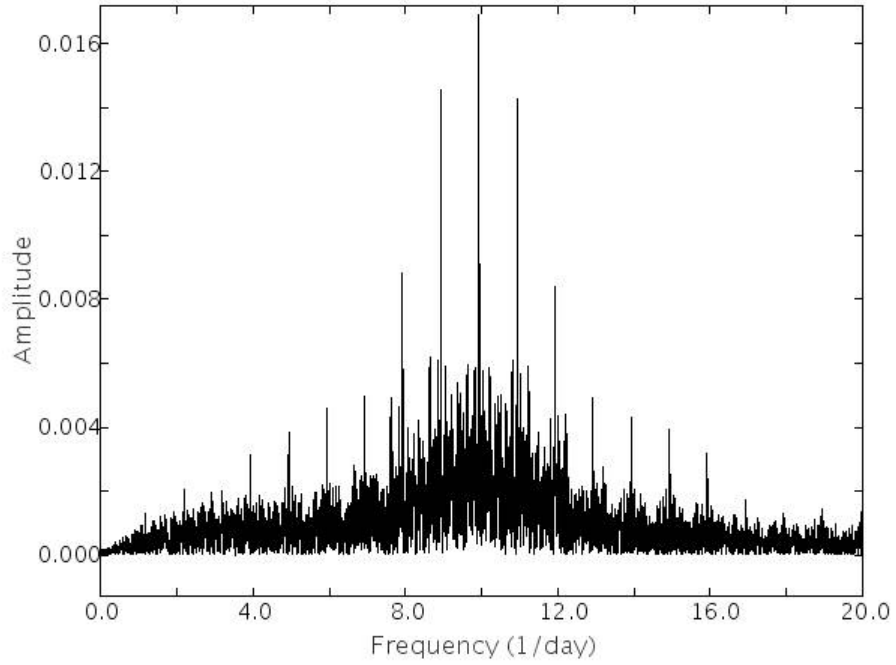

(b)

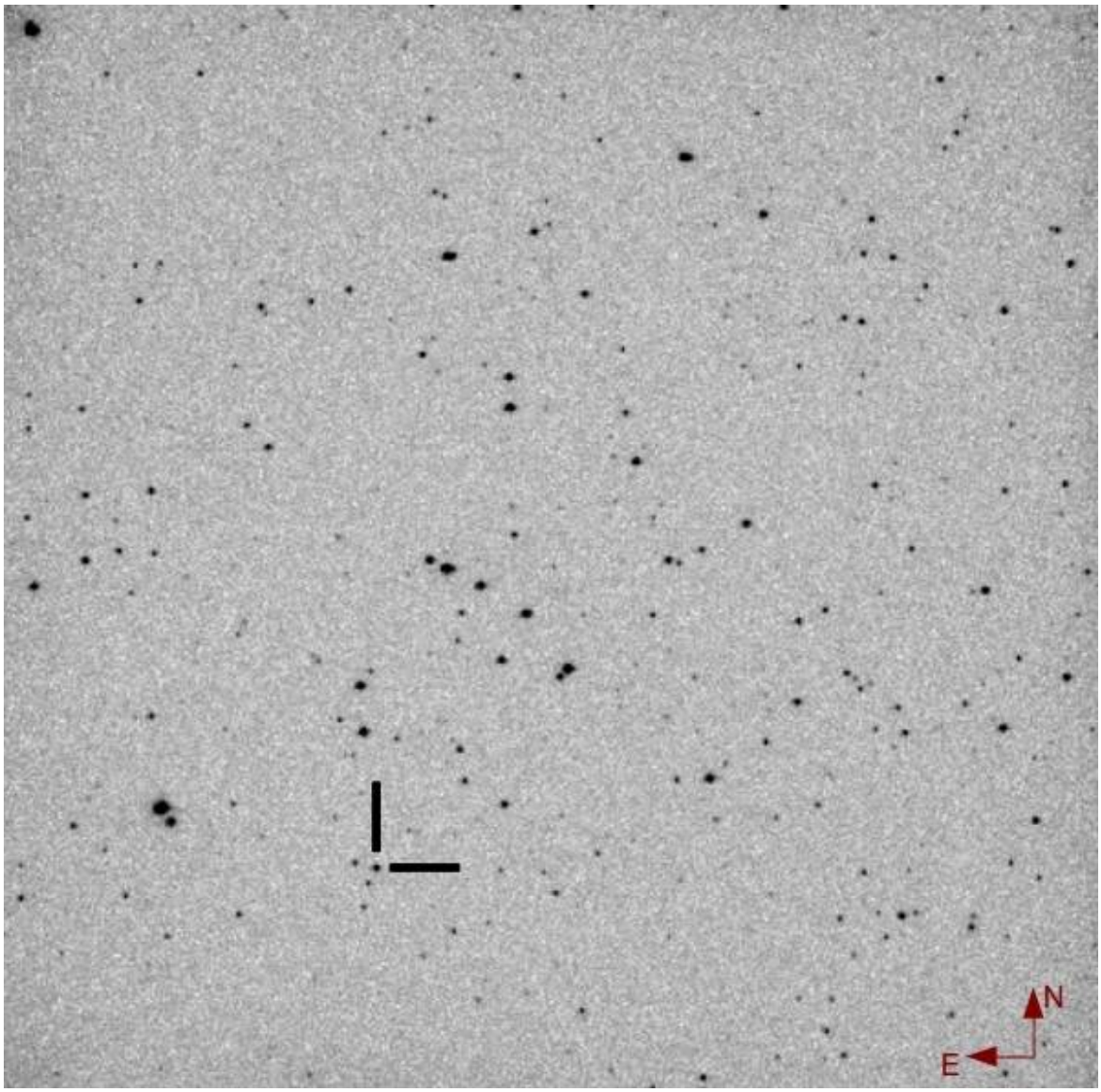

(c)